

CARBON AND OXYGEN ISOTOPE FRACTIONATION IN
LABORATORY-PRECIPIATED, INORGANIC CALCITE

by

EVAN BRUCE BAKER

A THESIS

Presented to the Department of Geological Sciences
and the Graduate School of the University of Oregon
in partial fulfillment of the requirements
for the degree of
Master of Science

June 2015

THESIS APPROVAL PAGE

Student: Evan Bruce Baker

Title: Carbon and Oxygen Isotope Fractionation in Laboratory-Precipitated,
Inorganic Calcite

This thesis has been accepted and approved in partial fulfillment of the requirements
for the Master of Science degree in the Department of Geological Sciences by:

James Watkins	Chair
Mark Reed	Member
Ilya Bindeman	Member

and

Scott L. Pratt	Dean of the Graduate School
----------------	-----------------------------

Original approved signatures are on file with the University of Oregon Graduate
School.

Degree awarded June 2015.

© 2015 Evan Bruce Baker

THESIS ABSTRACT

Evan Bruce Baker

Master of Science

Department of Geological Sciences

June 2015

Title: Carbon and Oxygen Isotope Fractionation in Laboratory-Precipitated, Inorganic Calcite

Carbon and oxygen isotopes in calcite crystals provide a record of the environmental conditions under which the crystals formed. To investigate the influence of temperature, pH, and growth rate on isotope discrimination by calcite, we measured carbon and oxygen isotope fractionation through a series of calcite precipitation experiments at $T = 25^{\circ}\text{C}$ and $\text{pH} = 7.5 - 9.3$. We observe that neither the carbon nor oxygen isotope compositions correspond to the theoretical equilibrium isotope fractionation between calcite and solution. We also demonstrate that the fractionation of oxygen isotopes between calcite and water decreases with increasing pH, consistent with available data from experiments in which the enzyme carbonic anhydrase was used. Finally, we compare the carbon and oxygen isotopes of our calcite crystals to those of biogenic carbonates.

This thesis includes previously unpublished co-authored material.

CURRICULUM VITAE

NAME OF AUTHOR: Evan Bruce Baker

GRADUATE AND UNDERGRADUATE SCHOOLS ATTENDED:

University of Oregon, Eugene
University of North Carolina at Chapel Hill

DEGREES AWARDED:

Master of Science, Geological Sciences, 2015, University of Oregon
Bachelor of Science, Geological Sciences, 2013, University of North Carolina at
Chapel Hill

PROFESSIONAL EXPERIENCE:

Graduate Teaching Fellow, Department of Geological Sciences, University of
Oregon, Eugene, 2013-2015

Field Geologist (intern), Cascades Volcano Observatory, U.S. Geological Survey,
Vancouver, Washington, 2013

Laboratory Technician, Isotope Geochemistry and Geochronology Laboratory,
University of North Carolina at Chapel Hill, 2011-2013

AWARDS AND HONORS:

Johnston Fellowship, Department of Geological Sciences, University of Oregon,
2013

UNC Chancellor's Award, Op White Prize in Geology, University of North
Carolina at Chapel Hill, 2013

Honors and Highest Distinction, University of North Carolina at Chapel Hill, 2013

ACKNOWLEDGMENTS

I wish to thank my advisor James Watkins and my committee members Mark Reed and Ilya Bindeman for their excellent advising. Special thanks to Jim Palandri for his enthusiastic technical assistance. Andrew Ross and Jennifer McKay of the CEOAS stable isotope laboratory at Oregon State University provided the stable isotope measurements. Lev Zakharov and John Donovan at the Lorry I. Lokey Laboratory helped determine the mineralogy of the precipitates. This research was supported by the University of Oregon through startup funds to JMW.

TABLE OF CONTENTS

Chapter	Page
I. OVERVIEW	1
II. CARBON AND OXYGEN ISOTOPE FRACTIONATION IN LABORATORY-PRECIPIATED, INORGANIC CALCITE	2
APPENDICES	
A. EXPERIMENT SUMMARIES	22
B. SEM IMAGES	36
C. XRD SPECTRA	38
D. UNCERTAINTY IN CARBON ISOTOPE FRACTIONATION	40
REFERENCES CITED	42

LIST OF FIGURES

Figure	Page
1. Carbon and oxygen isotopes in the carbonate system.	5
2. Schematic of the apparatus used for the inorganic calcite precipitation experiments.	10
3. Monitoring data showing the behavior of a typical experiment.	12
4. Carbon isotope fractionation between calcite and HCO_3^- as a function of pH.	15
5. Oxygen isotope fractionation between calcite and water as a function of pH.	15
6. Carbon and oxygen isotope fractionation measured in inorganic calcite compared to the fractionation in biogenic calcite.	19

LIST OF TABLES

Table	Page
1. Data Summary.	14
2. Sampling Data.	22

CHAPTER I

OVERVIEW

The body of this thesis is original research prepared for submission to *Earth and Planetary Science Letters* with Dr. James Watkins as coauthor. The appendices contain additional information.

Dr. Watkins contributed editorial support throughout and original material to the clumped isotope discussion (section 5.4). The rest of the work presented here, including the experiments, data analysis, and interpretation is my own.

CHAPTER II

CARBON AND OXYGEN ISOTOPE FRACTIONATION IN LABORATORY-PRECIPIATED, INORGANIC CALCITE

1. Introduction

The fractionation of stable isotopes between seawater and marine carbonates is dependent on numerous environmental variables at the time of carbonate crystal growth. For oxygen isotopes, the fractionation is strongly temperature-dependent (Urey, 1947; McCrea, 1950), making oxygen isotopes in carbonate the predominant proxy for ocean paleo-temperature reconstructions. Carbon isotopes, in contrast, are fractionated between calcite and dissolved carbon mainly by biological processes such as photosynthesis, which preferentially enriches the organism in heavy carbon (^{13}C). Thus, carbon isotopes have served as a proxy for biologic productivity by linking the carbon isotope composition of marine carbonates to the abundance of photosynthesizing organisms in the oceans (Zeebe, 2001).

Geochemical studies of inorganic calcite tend to focus exclusively on either carbon or oxygen isotope systematics, perhaps overlooking how isotopic fractionation of these two elements might be inter-related. The reasons for this have to do with the assumption that isotopic fractionation between calcite and aqueous solution occurs under near-equilibrium conditions. For oxygen isotopes, the equilibrium fractionation factor is independent of solution pH because most oxygen is housed in H_2O molecules (Deines, 2005), whereas for carbon isotopes, the equilibrium fractionation factor varies with pH because all of the carbon is stored in dissolved inorganic carbon ($\text{DIC} = \text{CO}_2 + \text{HCO}_3^- + \text{CO}_3^{2-}$) (Romanek et al., 1992; Zeebe and Wolf-Gladrow, 2001). The assumption of equilibrium implies that the final isotopic compositions of the exchanging phases (calcite and aqueous solution) depends primarily on the vibrational energies of molecules in the exchanging phases and is therefore independent of reaction mechanisms or pathways.

Several recent studies, however, have made a compelling case that equilibrium is not attained in many natural and experimental settings (Coplen, 2007; Dietzel et al., 2009; Watkins et al., 2013, 2014). When minerals grow in a non-equilibrium regime, the reaction mechanisms (i.e., the physical transport of isotopes by diffusion and reaction to the mineral lattice) become important considerations when interpreting

the mineral’s stable isotope composition. For the mineral calcite, the current thinking is that crystal growth proceeds via the attachment of Ca^{2+} , HCO_3^- and CO_3^{2-} ions to the mineral surface. Since HCO_3^- and CO_3^{2-} have different carbon and oxygen isotope compositions (Zeebe and Wolf-Gladrow, 2001; Beck et al., 2005), the carbon and oxygen isotope composition of calcite should depend on the relative proportions of HCO_3^- and CO_3^{2-} participating in crystal growth.

The isotopes of carbon (^{12}C and ^{13}C) and the isotopes of oxygen (^{16}O , ^{17}O , and ^{18}O) can be combined in a myriad of ways to form a catalog of isotopically-distinct molecules, or isotopologues, of HCO_3^- and CO_3^{2-} . If calcite were indeed to grow by the attachment of ‘long-lived’ molecules of (bi-)carbonate anions, then the isotope effects for oxygen should be twice that for carbon since the change in mass of $^{12}\text{C}^{16}\text{O}^{16}\text{O}^{16}\text{O}$ upon ^{18}O -substitution (2 amu’s) is twice the change in mass upon ^{13}C substitution (1 amu). Testing such a hypothesis requires experiments where (1) the carbon and oxygen isotope composition of HCO_3^- and CO_3^{2-} are unchanging during the crystal growth process and (2) carbon and oxygen isotopic fractionation factors are measured on the same sets of aqueous solution and crystals. Prior to this work, there were no experiments for which both criteria were satisfied.

There is only one experimental study on inorganic calcite for which carbon isotope fractionation factors were reported (Romanek et al., 1992), but those experiments span a range in pH (6.62 to 7.75) that is below the range of interest to many investigators. By contrast, there have been many experimental studies that have focused on oxygen isotope systematics, but the results have been variable, and in some ways conflicting, due in part to experimental details that give rise to non-constant isotopic compositions of HCO_3^- and CO_3^{2-} during calcite growth.

In this study we present carbon and oxygen isotope fractionation data for inorganic calcite crystals grown from an isotopically equilibrated solution at constant temperature, pH, and growth rate. The experiments are designed to keep the carbon and oxygen isotope composition of DIC constant and enable us to isolate the effect of pH on both carbon and oxygen isotopes. We use this information to deduce important parameters for existing crystal growth models and for comparison to biogenic carbonates to improve the assessment of biological influences on isotope uptake. The specific questions that our study is designed to address are:

- What is the pH dependence of carbon and oxygen isotope discrimination by calcite?
- Do HCO_3^- and CO_3^{2-} behave as ‘long-lived’ building blocks of calcite?
- How and why does isotope fractionation in biogenic calcite differ from that in inorganic calcite?
- Are non-equilibrium ‘clumped’ isotope effects caused by isotopic disequilibrium among DIC species?

2. General Principles and Notation

2.1 Speciation and isotope fractionation in carbonate

Carbon dioxide exists as four separate species in solution: carbonic acid (H_2CO_3), aqueous carbon dioxide ($\text{CO}_{2(\text{aq})}$), bicarbonate ion (HCO_3^-), and carbonate ion (CO_3^{2-}). H_2CO_3 and $\text{CO}_{2(\text{aq})}$ are not chemically separable and are reported together here as CO_2 (after Zeebe and Wolf-Gladrow (2001)). The sum of the dissolved species is called total dissolved inorganic carbon (DIC). The pH of the solution and the proportions of the various dissolved species are interrelated, in that as pH increases the predominant dissolved species changes from CO_2 to HCO_3^- , and then from HCO_3^- to CO_3^{2-} (Fig. 1a). The equilibrium isotope fractionation between each of the DIC species is shown in Figs. 1b and 1c. The isotope composition of DIC at a given pH is an average of the isotopic compositions of the individual DIC species, weighted by the relative abundance of those species at that pH.

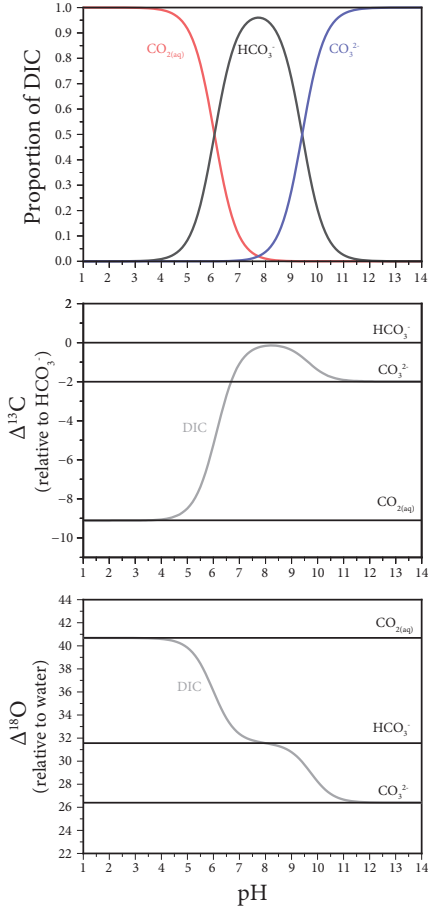


Figure 1: Carbon and oxygen isotopes in the carbonate system. *Top:* Bjerrum plot. The abundance of each of the DIC species is dependent on solution pH. In the pH range of our experiments (7.50 to 9.30), HCO_3^- is always the most abundant species, with CO_3^{2-} becoming a significant fraction of DIC only in the higher pH experiments. *Middle:* Carbon isotope composition of individual dissolved carbon species and total DIC relative to HCO_3^- . The equilibrium fractionation of DIC approaches different DIC species as those become the predominant species in solution. *Bottom:* Oxygen isotope composition of individual dissolved carbon species and total DIC relative to water. Again, the equilibrium fractionation of DIC reflects the relative proportions of DIC species in solution.

2.2 Principles of CaCO_3 precipitation

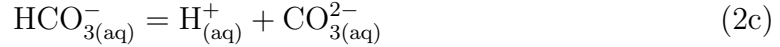
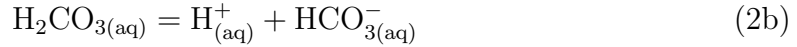
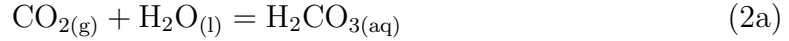
The growth or dissolution of calcium carbonate depends on the concentration of dissolved Ca^{2+} and CO_3^{2-} ions in aqueous solution. Calcite will tend to precipitate from a solution that is supersaturated, where the degree of supersaturation (Ω) is defined as:

$$\Omega = \frac{[\text{Ca}^{2+}][\text{CO}_3^{2-}]}{K_{\text{sp}}}. \quad (1)$$

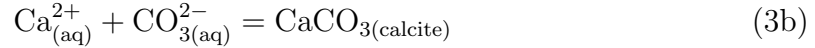
The solubility product, K_{sp} , is dependent on the temperature and salinity of the solution and has a value of 2.05×10^{-8} in our experiments (based on equations in Zeebe and Wolf-Gladrow, 2001). A solution is supersaturated when $\Omega > 1$ and undersaturated when $\Omega < 1$. However, to overcome energy barriers required to nucleate new crystals, the solution needs to be *critically* supersaturated (i.e., $\Omega \geq \Omega_{\text{crit}}$). Assuming K_{sp} is constant, there are several ways to reach critical supersaturation: (1) Add

Ca²⁺ to the solution, (2) add dissolved inorganic carbon (DIC) at constant pH, (3) increase pH at constant [DIC] to increase the proportion of DIC in the form of CO₃²⁻, and (4) increase pH by degassing CO₂ (changing [DIC]). The latter process involves the competing effects of decreasing [DIC] but increasing the proportion of DIC that is in the form of CO₃²⁻. In our experiments, DIC is added to the solution (at constant pH) by bubbling CO_{2(g)}:

Step 1 – CO₂ dissolves in solution:



Step 2 – CaCO₃ precipitates from solution:



We distinguish between equations 3a and 3b to emphasize that both HCO₃⁻ and CO₃²⁻ participate in calcite growth.

2.3 Isotope Notation

We report carbon and oxygen isotope fractionation with Δ notation:

$$\Delta^{18}\text{O}_{\text{xtl-w}} = 1000 \times \ln(\alpha_{\text{xtl-w}}), \quad (4a)$$

and

$$\Delta^{13}\text{C}_{\text{xtl-DIC}} = 1000 \times \ln(\alpha_{\text{xtl-DIC}}), \quad (4b)$$

where the fractionation factors (α) are defined as:

$$\alpha_{\text{xtl-w}} = \frac{\delta^{18}\text{O}_{\text{calcite}} + 1000}{\delta^{18}\text{O}_{\text{water}} + 1000}, \quad (5a)$$

and

$$\alpha_{\text{xtl-DIC}} = \frac{\delta^{13}\text{C}_{\text{calcite}} + 1000}{\delta^{13}\text{C}_{\text{DIC}} + 1000}. \quad (5b)$$

The δ values represent carbon and oxygen isotope compositions expressed relative to a standard:

$$\delta^{13}\text{C}_{\text{xtl}} = \left(\frac{{}^{13}\text{C}/{}^{12}\text{C}_{\text{calcite}}}{{}^{13}\text{C}/{}^{12}\text{C}_{\text{standard}}} - 1 \right) \times 1000, \quad (6\text{a})$$

$$\delta^{13}\text{C}_{\text{DIC}} = \left(\frac{{}^{13}\text{C}/{}^{12}\text{C}_{\text{DIC}}}{{}^{13}\text{C}/{}^{12}\text{C}_{\text{standard}}} - 1 \right) \times 1000, \quad (6\text{b})$$

$$\delta^{18}\text{O}_{\text{xtl}} = \left(\frac{{}^{18}\text{O}/{}^{16}\text{O}_{\text{calcite}}}{{}^{18}\text{O}/{}^{16}\text{O}_{\text{standard}}} - 1 \right) \times 1000, \quad (6\text{c})$$

and

$$\delta^{18}\text{O}_{\text{w}} = \left(\frac{{}^{18}\text{O}/{}^{16}\text{O}_{\text{w}}}{{}^{18}\text{O}/{}^{16}\text{O}_{\text{standard}}} - 1 \right) \times 1000. \quad (6\text{d})$$

We report $\delta^{13}\text{C}_{\text{xtl}}$ and $\delta^{13}\text{C}_{\text{DIC}}$ relative to Vienna Pee Dee Belemnite (VPDB) and $\delta^{18}\text{O}_{\text{xtl}}$ and $\delta^{18}\text{O}_{\text{w}}$ relative to Vienna Standard Mean Ocean Water (VSMOW).

2.4 Experimental challenges

There are many considerations that go into designing a crystal growth experiment that can answer the questions specific to a given study. Since we are interested in isolating the effects of pH, temperature, and growth rate on the carbon and oxygen isotopic composition of calcite, it is important that these variables are well-controlled. Although numerous studies have grown calcite in the laboratory for paleoproxy calibrations, most studies have not controlled pH or growth rate because the equilibrium oxygen isotope fractionation between calcite and water should be independent of both pH and growth rate (Watson, 2004; Deines, 2005). The fact that such dependencies have been observed, however, shows that many previous measurements of oxygen isotope fractionation factors are not representative of true equilibrium. This may also be true for carbon isotopes.

Since the growth of calcite involves the attachment of dissolved HCO_3^- and CO_3^{2-} anions to Ca^{2+} sites on a crystal surface, there are a couple ways that non-equilibrium effects may arise in a calcite growth experiment: (1) isotopic disequilibrium among

DIC species and/or (2) isotopic fractionation due to transport of DIC anions to, or from, the mineral surface. For the former, the isotope exchange experiments of Beck et al. (2005) showed that the kinetics of oxygen isotope equilibration between DIC and water are typically too slow to keep pace with the rapid growth rates of laboratory experiments, meaning that in most experiments calcite likely inherits oxygen isotopes from an unequilibrated DIC pool. Notably, addition of the enzyme carbonic anhydrase has been shown to dramatically decrease oxygen isotope equilibration times from several hours to just a few minutes (Uchikawa and Zeebe, 2012; Watkins et al., 2013). Carbonic anhydrase is present in the cells of all known organisms and plays a role in maintaining cell pH by catalyzing the hydration of CO_2 ($\text{CO}_{2(\text{aq})} + \text{H}_2\text{O} = \text{HCO}_3^- + \text{H}^+$) (Kupriyanova and Pronina, 2011). For our purposes, the catalysis of this reaction is an essential tool for maintaining oxygen isotope equilibration in our growth solution. Unfortunately, carbonic anhydrase loses effectiveness as pH increases because hydroxylation replaces hydration as the predominant exchange reaction (Uchikawa and Zeebe, 2012; Watkins et al., 2013). Therefore, calcite growth experiments at approximately pH 10 or higher will need to employ a different method to equilibrate oxygen isotopes.

A catalyst is not necessary for carbon because equilibration of carbon isotopes between DIC species occurs in under 30 seconds (Zeebe et al., 1999). The carbon isotope pool, however, presents a different challenge. Because there is a limited amount of carbon in solution (compared to the virtually unlimited supply of oxygen in H_2O), experiments that start with a fixed DIC concentration will deplete a significant fraction of that pool as calcite precipitates. This means that $\delta^{13}\text{C}_{\text{DIC}}$ will drift during the experiment, making it difficult to determine carbon isotope fractionation factors between calcite and DIC. A continuous supply of DIC is necessary to constantly replenish the DIC pool and hold $\delta^{13}\text{C}_{\text{DIC}}$ steady during the crystal growth period. This is where the experiments presented herein are unique.

3. Experimental Methods

3.1 Experiment overview

In our experiments, dissolved inorganic carbon (DIC) is added to a Ca-bearing aqueous solution by CO_2 bubbling. When the concentrations of dissolved Ca^{2+} and DIC (as mainly HCO_3^- and CO_3^{2-}) reach a critical super-saturation, calcite crystals (CaCO_3) nucleate spontaneously and grow on the container walls. A key aspect

of this experimental approach is that the $\delta^{13}\text{C}$ of DIC is relatively constant throughout the crystal growth period, because there is a continuous supply of DIC from the CO_2 -bearing bubbles. Carbonic anhydrase, an enzyme promoting rapid equilibration of isotopes between DIC and water, is added to ensure that the solution remains in isotopic equilibrium during calcite growth (Uchikawa and Zeebe, 2012; Watkins et al., 2013). Environmental variables such as temperature, pH, and alkalinity are also controlled and monitored throughout the experiment. With this setup we are able to precipitate inorganic calcite crystals under controlled conditions from a solution in which HCO_3^- and CO_3^{2-} have known isotopic compositions.

3.2 Experiment apparatus

A diagram of our apparatus is provided in Figure 2. Approximately 1450 mL of starting solution (15 mM CaCl_2 and 5 mM NH_4Cl dissolved in 18 M Ω distilled and deionized water) is poured into the experimental beaker. An additional 10 mL containing 10-25 mg of dissolved bovine carbonic anhydrase is also added to the solution shortly before the start of each experiment.

The experimental beaker is immersed in a larger water bath to control temperature. A heating element is inserted into this surrounding water bath along with a thermocouple for monitoring the temperature. Temperature in each experiment was controlled to $25.0 \pm .2^\circ\text{C}$. The water bath and the experimental beaker within are then set on a magnetic stir plate. We set this to spin a magnetic stir bar inside the experimental beaker at 400 rpm, ensuring that the solution stays well mixed.

The experimental beaker is sealed with a cap that includes several ports for inputs and outputs. A diffusion stone (pore size: 2 μm) delivers microbubbles of a N_2 - CO_2 gas mixture to the solution at a constant rate. To keep growth rates relatively constant between experiments at different pH, we adjust the flux of CO_2 into the solution by changing the flow rate of the gas and by using gas tanks with different concentrations of CO_2 . In most experiments, the rate of addition of CO_2 to solution is 0.12 mmols/h. In the apparatus headspace, a long, thin outlet tube lets gas slowly exit into a separate chamber containing a CO_2 probe, allowing us to monitor the proportion of CO_2 reaching the headspace after traveling through solution. The positive pressure of the constant CO_2 input prevents outside air from back-flowing through the outlet into the experiment. An auto-titration tube adds NaOH during the experiment to maintain constant pH as calcite precipitates, and a pH probe monitors the pH of the solution and communicates with the auto-titrator. A port for

connecting a syringe is used to collect solution samples, allowing us sample $\delta^{13}\text{C}$ of DIC and $\delta^{18}\text{O}$ of water throughout an experiment.

A glass disc set in the experimental beaker becomes coated with crystals over the course of an experiment and can be easily removed afterwards for obtaining SEM images of the precipitates (see Appendix). The rest of the crystals are dried in the fume hood and then collected from the walls of the beaker using a plastic spatula. This experimental setup allows us to control, monitor, and sample the precipitation environment throughout the entire crystal growth period and compare solution composition with the composition of the bulk calcite crystals collected afterwards.

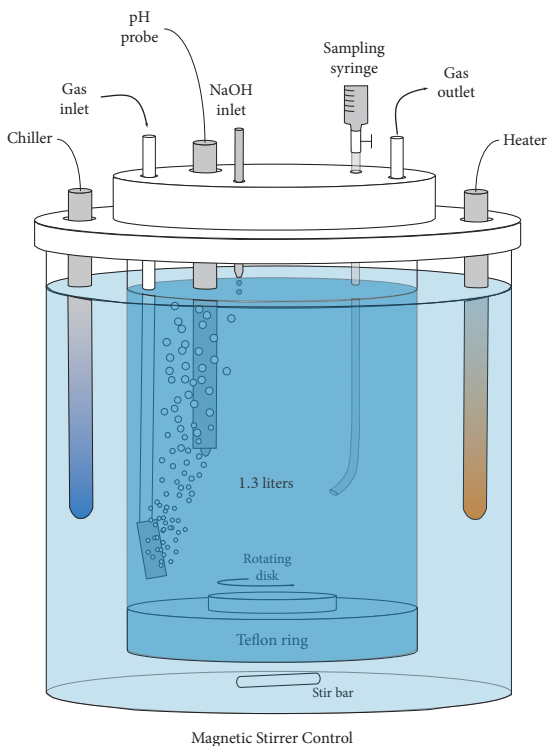


Figure 2: Schematic of the apparatus used for the inorganic calcite precipitation experiments. The outer vessel is a constant temperature bath. The inner vessel houses the aqueous solution (15 mM CaCl_2 + 5 mM NH_4Cl) from which calcite is precipitated. The lid of inner vessel has multiple ports for monitoring the experiment (see text for explanation). Modified from Watkins et al. (2013).

3.3 Experiment progression

Before an experiment begins, the N_2 - CO_2 gas mixture is bubbled into the sealed beaker containing the starting solution, so that the gas mixture can replace the original headspace of the container. The progress of the headspace replacement is monitored by the CO_2 probe, which initially reads ~ 400 ppm CO_2 (the concentration in the laboratory air) and then gradually drops to 200 ppm (the concentration in the

gas tank). The initial pH of the starting solution is ~ 5.0 and typically increases to ~ 5.5 as the $\text{N}_2\text{-CO}_2$ gas mixture is bubbled in (pH *increases* with addition of our CO_2 gas because the CO_2 is *less concentrated* in our $\text{N}_2\text{-CO}_2$ gas mixture than in the laboratory air). When the headspace is fully replaced, the experiment can begin.

The experiment begins when the auto-titrator is switched on and the pH is increased to the specified setpoint by NaOH addition. As auto-titration raises the pH to the setpoint, the concentration of CO_2 in the headspace drops dramatically (due to uptake of additional $\text{CO}_{2(\text{g})}$ by the solution as $\text{CO}_{2(\text{aq})}$ converts to $\text{HCO}_{3(\text{aq})}^-$ and $\text{CO}_{3(\text{aq})}^{2-}$ at higher pH) and then stabilizes for the duration of the experiment. In the first phase of the experiment (before precipitation), the concentration of DIC builds up in solution, increasing the degree of super-saturation with respect to calcite. $\delta^{13}\text{C}_{\text{DIC}}$ also increases as the heavier carbon is fractionated into solution while the lighter carbon reaches the headspace. Calcite begins to nucleate spontaneously when the solution becomes critically supersaturated. Note that the critical supersaturation varies with pH, from $\Omega_{\text{crit}} \approx 10$ at pH 8.3 to $\Omega_{\text{crit}} \approx 30$ at pH 9.3.

In the second phase of the experiment, calcite precipitates at a constant rate, quickly pulling out the heaviest carbon and thereby lowering $\delta^{13}\text{C}_{\text{DIC}}$. $\delta^{13}\text{C}_{\text{DIC}}$ stabilizes rapidly after the onset of calcite precipitation, providing an approximately constant isotopic reservoir for the majority of the precipitation period. The [DIC] drops gradually during calcite precipitation, indicating that calcite growth slightly outpaces the rate of DIC addition. The output from a typical experiment is shown in Figure 3.

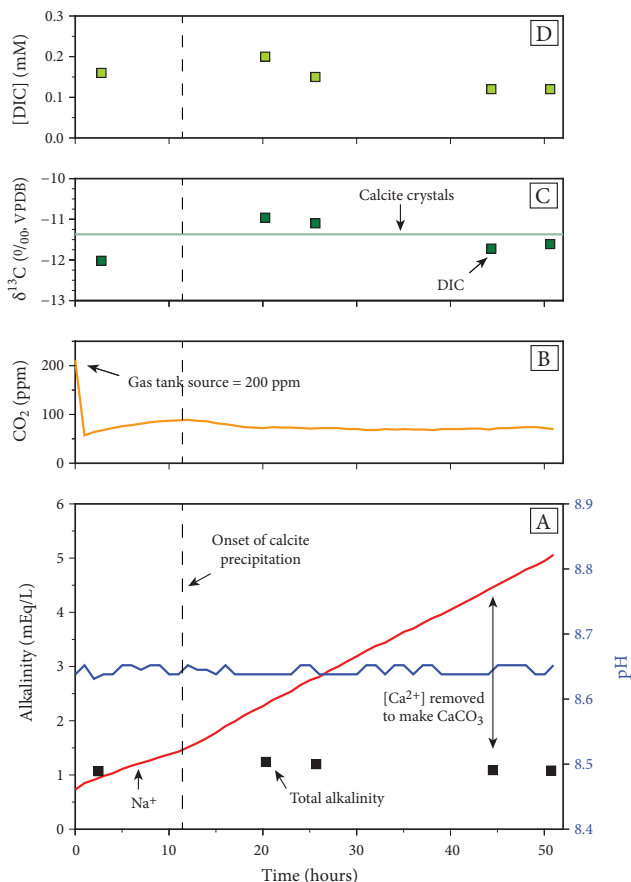


Figure 3: Monitoring data showing the behavior of a typical experiment (Experiment 8, $T = 25^{\circ}\text{C}$, $\text{pH} = 8.65$). (A) $[\text{Na}^+]$ increases as NaOH is added to keep pH constant during the experiment. The amount of Na added is proportional to the amount of calcite precipitated. The bend in the NaOH curve at ~ 12 hours marks the onset of calcite precipitation. Total alkalinity and pH are constant during crystal growth. (B) Concentration of $\text{CO}_{2(g)}$ in the apparatus headspace after the $\text{N}_2\text{-CO}_2$ gas mixture bubbles through solution. The rate of CO_2 input and the concentration of CO_2 in the headspace are constant during crystal growth. (C) $\delta^{13}\text{C}_{\text{DIC}}$ is relatively constant during crystal growth. $\delta^{13}\text{C}_{\text{xtl}}$ is fractionated from $\delta^{13}\text{C}_{\text{DIC}}$. Error bars on this analysis are smaller than the symbol size. (D) Concentration of DIC measured in solution.

3.4 Isotope measurements

The isotope compositions of dissolved inorganic carbon (DIC), water, and calcite precipitate were measured in the CEOAS stable isotope laboratory at Oregon State University. Data are presented in standard delta notation relative to VPDB for DIC and $\delta^{13}\text{C}_{\text{xtl}}$ and relative to VSMOW for water and $\delta^{18}\text{O}_{\text{xtl}}$. The calcite crystals were reacted with $\sim 105\%$ orthophosphoric acid in a Kiel III preparation device. The resulting CO_2 gas was then transferred to a Finnigan/MAT 252 mass spectrometer for analysis. Instrumental precision is $\pm .03\text{‰}$ for $\delta^{13}\text{C}$ and $\pm .05\text{‰}$ for $\delta^{18}\text{O}$. For $\delta^{13}\text{C}$ of DIC, 3.5 mL of solution was added by syringe through a rubber septa cap into a He-flushed, glass vial containing .1 mL of $\sim 85\%$ orthophosphoric acid. The samples

were allowed to equilibrate for over 24 hours and then analyzed by continuous-flow mass spectrometry using a GasBench-DeltaV system. Precision for this analysis is $\pm .15\%$. The approximate [DIC] in solution is obtained by comparing the CO₂ signal produced by the solution samples to that produced by an in-house DIC standard run multiple times in every batch of samples. The $\delta^{18}\text{O}$ of water was analyzed using the CO₂-equilibration method (5 ml H₂O equilibrated with CO₂ for 10 hours at 18°C while shaken) and measured by dual inlet mass spectrometry on the DeltaPlus XL. Precision is $\pm .05\%$.

4. Results

Results from 12 precipitation experiments at 25°C in the pH range 7.5 to 9.3 are reported in Table 1. Growth rate is controlled and varies from $10^{-6.0}$ to $10^{-6.6}$ mol/m²/s between experiments. We did not attempt to vary the growth rate to test the rate dependence, because the effect of growth rate on $\Delta^{13}\text{C}_{\text{xtl-DIC}}$ and $\Delta^{18}\text{O}_{\text{xtl-w}}$ has been shown to be small over the range of rates accessible with laboratory experiments (Romanek et al., 1992; Watkins et al., 2014)). Mid-experiment sampling of $\delta^{13}\text{C}_{\text{DIC}}$ and $\delta^{18}\text{O}_{\text{w}}$ confirms that the compositions of the carbon and oxygen isotope reservoirs were relatively steady during the crystal growth period (see Fig. 3 and Appendix A). The mineralogy of the precipitates in each experiment was checked by X-ray diffraction (XRD)(see Discussion for comments on vaterite co-precipitation in experiments 9, 10, and 11). Scanning electron microscope (SEM) images of crystals precipitated in each experiment are included in the Appendix.

The $\Delta^{13}\text{C}_{\text{xtl-HCO}_3^-}$ and $\Delta^{18}\text{O}_{\text{xtl-w}}$ fractionation factors are plotted against the pH of the growth solution in Figures 4 and 5, respectively. We compare our results to the equilibrium fractionations of dissolved carbon species in solution (Usdowski and Hoefs, 1993; Zeebe and Wolf-Gladrow, 2001; Zeebe, 2007), the published calcite equilibrium fractionations (Bottinga, 1968; Coplen, 2007), and the precipitates of similar studies (Romanek et al., 1992; Watkins et al., 2014).

Table 1: Data Summary

Exp. #	pH	CO ₂ flow ⁽¹⁾ (mmols/h)	Time (h)	log ₁₀ <i>R</i> ⁽²⁾ (mol/m ² /s)	Δ ¹³ C _{x_{tl}-DIC} ⁽³⁾ (VPDB)	Δ ¹⁸ O _{x_{tl}-w} ⁽⁴⁾ (VSMOW)	Min. ⁽⁵⁾
14	7.50	1.20	44.5	-6.11	0.33	28.38	cal.
15	7.50	0.60	44.8	-6.06	0.19	28.23	cal.
3	8.30	0.12	66.6	-6.38	0.27	27.99	cal.
4	8.30	0.12	93.7	-6.58	0.14	27.98	cal.
7	8.65	0.12	51.4	-6.31	-0.20	27.91	cal.
8	8.65	0.12	51.0	-6.29	-0.01	27.98	cal.
5	9.00	0.12	25.1	-5.98	-0.08	27.83	cal.
6	9.00	0.12	67.2	-6.32	-0.16	24.84 ⁽⁶⁾	cal.
9	9.30	0.12	26.8	-6.05	0.92	28.51	cal., vat.
10	9.30	0.12	27.4	-6.02	0.83	29.22	cal., vat.
11	9.30	0.05	46.7	-6.25	0.63	28.26	cal., vat.
12	9.30	0.05	50.9	-6.30	0.20	27.69	cal.

1. Rate at which CO_{2(g)} is bubbled into solution. About half of the incoming CO_{2(g)} is taken up by the solution (based on our headspace CO_{2(g)} monitoring data). Recall that pH is controlled by NaOH addition, not flow rate.

2. Estimated uncertainty in *R* is ± 0.12 log units due to uncertainty in the reactive surface area.

3. Estimated uncertainty in Δ¹³C_{x_{tl}-DIC} is ± 0.30 ‰.

4. Estimated uncertainty in Δ¹⁸O_{x_{tl}-w} is ± 0.10 ‰.

5. Mineralogy. cal. = calcite, vat. = vaterite.

6. We interpret this anomalously low Δ¹⁸O_{DIC-w} value to be the result of an experimental error.

Repeat experiments at pH 7.5, 8.3, 8.65, and 9.0 show good agreement, but there is significantly more scatter in Δ¹³C_{x_{tl}-DIC} and Δ¹⁸O_{x_{tl}-w} at pH 9.3. This scatter is caused by undesired precipitation of vaterite, a metastable CaCO₃ polymorph, in addition to calcite in some of our pH 9.3 experiments (confirmed by XRD in experiments 9, 10, and 11). This explains the anomalously high values of Δ¹⁸O_{x_{tl}-w} because vaterite oxygen isotope fractionation has been shown to be approximately 0.5‰ larger than that of co-precipitated calcite (Tarutani et al., 1969; Kim and O’Neil, 1997). The similar offset in our Δ¹³C_{x_{tl}-DIC} for those experiments suggests that *carbon* isotope fractionation in vaterite is also positively offset from that of calcite. Kim and O’Neil (1997) reported that calcite-vaterite mixtures were associated with high growth rates, so we decreased the growth rate in a repeat experiment (experiment 12) to prevent vaterite formation.

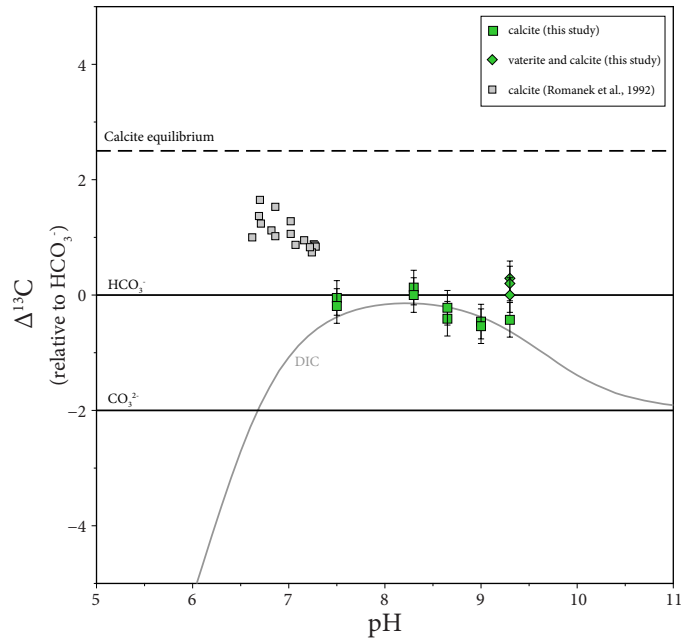


Figure 4: Carbon isotope fractionation between calcite and HCO_3^- as a function of pH. Equilibrium fractionations, relative to HCO_3^- , between calcite, dissolved carbon species, and total DIC are shown for reference. Watkins et al. (2014) did not report carbon isotope data for their precipitates.

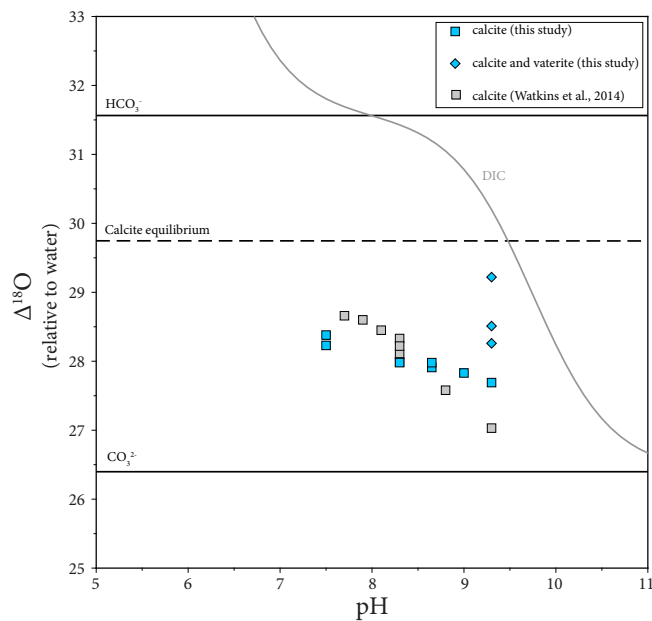


Figure 5: Oxygen isotope fractionation between calcite and water as a function of pH. Equilibrium fractionations, relative to water, between calcite, dissolved carbon species, and total DIC are shown for reference.

5. Discussion

5.1 What is the pH dependence of carbon and oxygen isotope discrimination by calcite?

The carbon and oxygen isotope fractionation factors between calcite and aqueous solution, $\Delta^{13}\text{C}_{\text{xtl-HCO}_3^-}$ and $\Delta^{18}\text{O}_{\text{xtl-w}}$, plot significantly below the theoretical equilibrium fractionation (Figs. 4 and 5), confirming that kinetic processes (such as diffusion and reaction) are affecting isotope partitioning in our precipitates. $\Delta^{13}\text{C}_{\text{xtl-HCO}_3^-}$ and $\Delta^{18}\text{O}_{\text{xtl-w}}$ both vary with pH, but show different relationships to the dissolved carbon species in solution.

5.1.1 Carbon

The carbon isotope composition of our precipitates is equal (within error) to the carbon isotope composition of DIC. In other words, $\Delta^{13}\text{C}_{\text{xtl-HCO}_3^-}$ is approximately equal to $\Delta^{13}\text{C}_{\text{DIC-HCO}_3^-}$, and $\Delta^{13}\text{C}_{\text{xtl-DIC}}$ is approximately zero (Fig. 4). There is therefore a significant discrepancy between our results and those of Romanek et al. (1992), which are positively offset from the equilibrium fractionation of HCO_3^- by about 0.5 ‰. Not only do the precipitates of Romanek et al. (1992) show a different fractionation than our precipitates, but they also appear to reflect the composition of an individual dissolved carbon species (such as HCO_3^-), rather than the composition of total DIC. We acknowledge that the similarity in isotope composition between total DIC and HCO_3^- in the pH range of our experiments makes it non-trivial to distinguish the relative contributions of DIC and HCO_3^- . However, the experimental results were highly reproducible and clearly follow the trend of DIC more closely than that of HCO_3^- .

The fact that the bulk $\delta^{13}\text{C}_{\text{xtl}}$ is indistinguishable from the average $\delta^{13}\text{C}_{\text{DIC}}$ in our experiments could lead some observers to conclude that our calcite crystals are consuming the entire DIC pool during precipitation. Complete precipitation of the DIC pool would force $\delta^{13}\text{C}_{\text{xtl}}$ to equal $\delta^{13}\text{C}_{\text{DIC}}$ and fractionation between crystal and DIC would be impossible to determine. However, our experimental setup precludes this scenario. We continually replenish the DIC pool by $\text{CO}_{2(\text{g})}$ bubbling, and mid-experiment sampling proves that DIC is available in solution throughout the precipitation phase. Also, in the experiments in which vaterite co-precipitated with calcite, the bulk fractionation is distinctly larger than DIC, which shows that precipitating phases *can* inherit a different isotopic composition than that of the DIC

reservoir. Thus, we emphasize that the our calcite crystals show the effects of kinetic fractionation rather than artifacts of the experiment.

The discrepancy between our results and those of Romanek et al. (1992) lead us to examine the differences between our experimental methods. Notably, Romanek et al. (1992) used seed crystals as nucleation sites for their precipitates, whereas we opt to critically super-saturate our growth solution to promote spontaneous nucleation. We would expect the process of accounting for the seed crystal in the Romanek et al. (1992) experiments to introduce considerable uncertainty, yet their dataset shows little scatter and we see no reason to disbelieve their results. Another difference is that our experiments utilize the enzyme carbonic anhydrase. Although the purpose of including carbonic anhydrase is to quicken the equilibration of *oxygen* isotopes (carbon isotope equilibration is thought to be rapid enough already), it is possible that carbonic anhydrase also has an effect on carbon isotope fractionation. Whether this is the case or not, carbonic anhydrase is undoubtedly present in the cells of calcifying marine organisms and its inclusion in calcite precipitation experiments is necessary to simulate precipitation in natural settings.

5.1.2 Oxygen

Oxygen isotope fractionation, $\Delta^{18}\text{O}_{\text{xtl-w}}$, decreases monotonically with increasing pH (Fig. 5). The trend in $\Delta^{18}\text{O}_{\text{xtl-w}}$ with increasing pH mirrors the trend of the DIC curve, but $\Delta^{18}\text{O}_{\text{xtl-w}}$ is smaller than $\Delta^{18}\text{O}_{\text{DIC-w}}$ by about 3 ‰. We see a slightly smaller pH dependence in our study than in Watkins et al. (2014), but overall, results from the two studies agree.

Of course, there are many more studies that have investigated kinetic fractionation of oxygen isotopes in calcite. For example Dietzel et al. (2009) reported $\Delta^{18}\text{O}_{\text{xtl-w}}$ values 2 to 5 ‰ smaller than ours and a stronger pH dependence. We can not compare our data directly to much of the existing literature, however, because those experiments were performed without carbonic anhydrase. The absence of carbonic anhydrase means that it is unlikely that the oxygen isotopes of dissolved carbon species were fully equilibrated in previous studies. Therefore, it is unclear how much of the final isotope fractionation between calcite and solution was affected by isotopic disequilibrium among dissolved species. How to test oxygen isotope fractionation at even higher pH remains an unsolved problem. Carbonic anhydrase loses effectiveness at high pH because hydroxylation, which is not catalyzed by carbonic anhydrase, replaces hydration as the dominant reaction mechanism between $\text{CO}_{2(\text{g})}$ and water.

5.2 Do HCO_3^- and CO_3^{2-} behave as ‘long-lived’ building blocks of calcite?

Calcite growth is thought to occur by the attachment of HCO_3^- and CO_3^{2-} to the mineral surface. If this is true, then carbon and oxygen atoms are delivered to the mineral surface together as part of a single DIC species, and therefore, we would expect to see similarities between carbon and oxygen isotope fractionation in calcite. However, our observation that the carbon isotope composition of calcite reflects that of DIC while the oxygen isotope composition is negatively offset from DIC suggests that calcite is not constructed by straightforward incorporation of DIC species. HCO_3^- and CO_3^{2-} molecules are composed of an inner carbon atom surrounded by oxygen atoms. At the mineral surface, oxygen atoms are more exposed to the solution, which may explain the fractionation from DIC in our oxygen isotope results (Wolthers et al., 2012).

Our results provide support for the idea that both HCO_3^- and CO_3^{2-} molecules are incorporated during calcite growth. The isotopic composition of DIC is determined by the relative proportions of $\text{CO}_{2(\text{aq})}$, HCO_3^- , and CO_3^{2-} in solution. Because the carbon and oxygen isotope composition of calcite reflects that of DIC, it follows that calcite must be built by each of the available DIC species. $\text{CO}_{2(\text{aq})}$ is not thought to contribute to calcite precipitation, and therefore we would not expect calcite to continue to mirror DIC at lower pH. In fact, this may be why our precipitates in experiments at pH 7.5 do not conform as closely to the DIC curve. At that pH, CO_3^{2-} is only 1% of the DIC pool and $\text{CO}_{2(\text{aq})}$ should not be influencing the isotopic composition. Thus we expect that calcite precipitated at even lower pH would incorporate only HCO_3^- and plot on the HCO_3^- line.

5.3 How and why does the isotopic discrimination of biogenic calcite differ from that of inorganic calcite?

Significant disagreement between published carbon and oxygen isotope fractionation factors motivated a search for other factors that could affect carbonate isotope uptake. McConnaughey (1989a,b) identified kinetic effects and vital effects as two processes that could offset $\Delta^{13}\text{C}_{\text{xtl-DIC}}$ and $\Delta^{18}\text{O}_{\text{xtl-w}}$ from their equilibrium values. As discussed above, kinetic effects are the result of non-equilibrium crystal growth, in which time-dependent processes like diffusion and reaction affect $\Delta^{13}\text{C}_{\text{xtl-DIC}}$ and $\Delta^{18}\text{O}_{\text{xtl-w}}$. Vital effects, on the other hand, arise from metabolic processes, such as photosynthesis and respiration, that occur within or around an individual organism. The term

also includes fractionation that may occur as dissolved carbon is moved across cell membranes in the organism.

Disentangling kinetics effects from vital effects has proven difficult in studies of biogenic carbonate because it is rarely clear whether offsets from equilibrium are due to kinetics or biology. The problem is further complicated by the observation that the magnitude of vital effects varies from species to species (Spero et al., 1997). In one of the few previous studies that tested the effect of pH on carbon and oxygen isotope fractionation in calcite, Spero et al. (1997) cultured foraminifera and found distinct fractionations between photosynthesizing and non-photosynthesizing organisms that could only be attributed to vital effects. When comparing our results with those of Spero et al. (1997), we see a striking distinction between the behavior of carbon and oxygen isotopes (Fig. 6). Whereas the pH dependence of oxygen isotope fractionation is in agreement for inorganic and biogenic calcite, carbon isotope fractionation is substantially lower in biogenic calcite than in inorganic calcite, at least for crystals precipitated above pH 8.3.

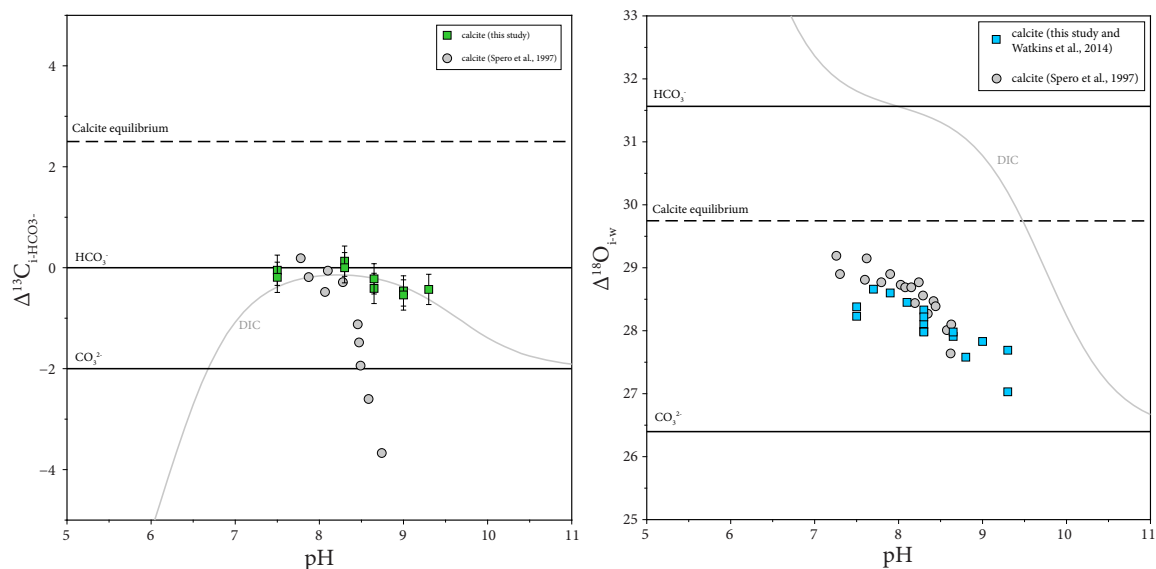


Figure 6: Carbon (*left*) and oxygen (*right*) isotope fractionation measured in the inorganic calcite of this study and in Watkins et al. (2014) ($\Delta^{18}\text{O}$ only, $\Delta^{13}\text{C}$ not reported) compared to the fractionation in the biogenic calcite of Spero et al. (1997). Results for oxygen are similar between inorganic and biogenic calcite, while carbon isotope fractionation behaves remarkably differently between the two.

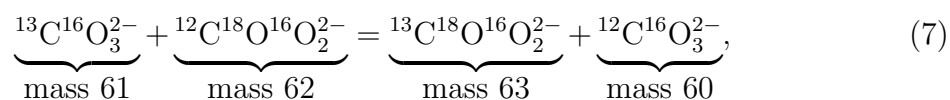
We hope that our results, which show that the carbon isotopic composition of inorganic calcite is indistinguishable from DIC and that the oxygen isotopic compo-

sition is offset from water across the pH range 7.50 to 9.30, will provide a baseline for the kinetic effect in inorganic calcite. With this baseline in place, deviations in the isotopic composition of calcifying organisms can be more definitively attributed to vital effects. Carpenter and Lohmann (1995), in a survey of carbon and oxygen isotopes in the calcite of brachiopod shells, illustrated the myriad issues posed by vital effects in biogenic carbonates when they reported not only inter-species differences, but also variation between different regions of individual shells. The use of any calcifying organism as a paleo-environment proxy, therefore, must first be supported by a thorough understanding of that organism’s calcifying mechanism. The products of this study provide an inorganic baseline, or expected value, to which species-specific vital effects can be compared.

It is possible that vital effects and kinetic effects work in concert to create the observed offsets. For example, McConnaughey (1989a) and Adkins et al. (2003) suggest that the inner DIC pool of corals is enriched in $\delta^{13}\text{C}$ by photosynthesis, and that this enrichment persists because the coral is calcifying faster than the hydration of $\text{CO}_{2(\text{aq})}$ can create isotopic equilibrium. Similarly, the pH of isolated DIC pools at the calcifying site may be significantly different than that of ambient seawater. In this way, biological processes could create kinetic offsets that are unusual for the known environmental conditions.

5.4 Are non-equilibrium ‘clumped’ isotope effects caused by isotopic disequilibrium among DIC species?

Clumped isotope geochemistry, or the study of bond-ordering within minerals or other phases, involves both carbon and oxygen isotope systematics. For carbonate molecules, the following isotope exchange reaction can be written (Ghosh et al., 2006):



which describes the extent to which the rare isotopes ^{13}C and ^{18}O are associated with each other as ‘clumps’ among the carbonate molecules. It is now possible for researchers to measure the relative abundance of the four isotopologues in the above reaction and it has been shown that the relative abundance varies systematically with temperature (Ghosh et al., 2006; Eiler, 2007, 2011). According to the above reaction, in which only the calcite phase is involved, one can infer the temperatures of car-

bonate formation from aqueous solution without requiring knowledge of the isotopic composition of the solution (Ghosh et al., 2006; Eiler, 2007, 2011). The assumption underlying this claim is that an equilibrium distribution of isotopologues is established. In cases where equilibrium is not established, clumped isotope compositions may in fact depend on reaction mechanisms that involve DIC species in the aqueous phase as well.

When different laboratories grow calcite at different temperatures to calibrate the oxygen isotope and clumped thermometers, they get slightly (but significantly) different results (Ghosh et al., 2006; Dennis and Schrag, 2010; Zaarur et al., 2013; Tang et al., 2014). In the absence of carbonic anhydrase, the timescale required for equilibrating the clumped isotope composition of the DIC pool is on the order of 10 hours at 25°C (Affek, 2013). It is therefore possible that the discrepancies between studies could be due a combination of factors, including (1) crystal growth from a non-equilibrated DIC pool, (2) drifting of the $\delta^{13}\text{C}$ of DIC, (3) drifting pH, (4) growth rate effects, and (5) other factors. The calcite crystals grown in this study are prime candidates for resolving some of these issues because, unlike most previous studies, we have knowledge of the carbon and oxygen isotope composition of DIC, we used carbonic anhydrase, we kept pH constant, and we have information on the growth rate of our crystals.

The clumped isotope compositions of our crystals will be measured at the University of Washington. We will investigate the temperature, pH, and growth rate dependence of isotopic clumping and compare the results to previous studies.

6. Conclusions

Calcite crystals were successfully precipitated in a controlled environment from an isotopically equilibrated solution at pH values from 7.50 to 9.30. These precipitates comprise the first experimental dataset for which the pH and isotopic equilibration of the growth solution was controlled and carbon and oxygen isotopes were measured on the same set of crystals. We find that pH variations have a measurable effect on the carbon and oxygen isotope composition of calcite, indicating that paleo-climate reconstructions may need to be adjusted to account for changes in ocean pH over geologic time. We also observe that whereas the pH dependence of oxygen isotope fractionation is similar for inorganic and biogenic calcite, carbon isotope fractionation behaves significantly differently between the two.

APPENDICES

Appendix A: Experiment summaries

Table 2: Sampling Data

Exp.#	time (h)	TA (meq/L)	[DIC] (mM)	$\delta^{13}\text{C}_{\text{DIC}}$ (VPDB)	$\delta^{18}\text{O}_w$ (VSMOW)
3	0.5	0.57	0.05	-10.08	-11.07
-	18.0	1.08	0.45	-7.70	-
-	22.5	0.85	0.25	-8.16	-
-	41.5	0.72	0.21	-9.89	-10.95
-	45.0	0.75	0.20	-10.00	-
-	66.5	0.74	0.18	-10.31	-10.93
4	0.5	0.53	0.10	-9.40	-11.01
-	21.0	0.91	0.36	-8.71	-10.99
-	27.5	0.78	0.25	-9.06	-
-	45.0	0.69	0.20	-10.22	-
-	50.5	0.68	0.22	-10.37	-10.91
-	74.0	0.73	0.21	-10.31	-
-	93.0	0.63	0.16	-10.55	-10.87
5	0.5	1.94	0.05	-12.46	-
-	19.0	1.94	0.15	-12.24	-10.97
-	25.0	1.92	0.13	-12.20	-10.94
6	1.0	1.65	0.04	-12.40	-11.03
-	24.5	2.04	0.25	-12.31	-
-	45.5	1.67	0.10	-12.55	-10.93
-	49.5	1.73	0.10	-12.73	-
-	67.0	1.67	0.06	-12.84	-10.91
7	3.0	1.17	0.11	-11.97	-11.92
-	20.5	1.17	0.19	-11.12	-
-	26.5	1.13	0.16	-11.26	-11.89
-	44.0	1.08	0.12	-11.53	-
-	51.0	1.10	0.11	-11.65	-11.82
8	2.5	1.07	0.16	-12.02	-11.84
-	20.5	1.24	0.20	-10.96	-11.83
-	25.5	1.20	0.15	-11.10	-
-	44.5	1.09	0.12	-11.72	-11.82
-	50.5	1.08	0.12	-11.61	-
9	2.5	2.87	0.16	-12.15	-11.93
-	20.5	2.61	0.08	-12.93	-11.86
-	24.0	2.59	0.07	-12.78	-
-	26.0	2.61	0.07	-12.70	-11.81

Table continued on next page.

Exp.#	time (h)	TA (meq/L)	[DIC] (mM)	$\delta^{13}\text{C}_{\text{DIC}}$ (VPDB)	$\delta^{18}\text{O}_w$ (VSMOW)
10	1.0	2.6	0.09	-12.10	-
-	3.5	2.9	0.18	-12.04	-12.00
-	23.5	2.6	0.07	-12.78	-11.89
-	27.0	2.6	0.06	-12.82	-11.86
11	1.0	2.70	0.33	-12.40	-11.92
-	20.0	2.62	0.08	-12.32	-
-	26.0	2.63	0.06	-12.07	-
-	45.0	2.55	0.04	-11.83	-11.86
-	46.5	-	0.05	-11.72	-
12	1.0	2.65	0.11	-12.54	-11.93
-	4.5	-	0.09	-13.25	-
-	21.0	2.51	0.05	-12.04	-
-	27.0	2.45	0.04	-11.96	-
-	46.0	2.48	0.04	-12.00	-
-	50.5	2.46	0.04	-12.08	-11.88
14	1.0	0.71	0.35	-9.97	-11.42
-	20.5	1.93	1.18	-3.84	-
-	23.0	-	1.22	-4.12	-
-	26.0	1.65	1.06	-4.61	-
-	44.0	1.46	1.06	-6.33	-11.28
15	2.0	0.93	0.51	-9.62	-11.44
-	21.5	1.87	1.29	-3.54	-
-	25.0	1.84	1.19	-3.52	-
-	44.5	1.53	0.96	-5.54	-11.32

Table continued from previous page.

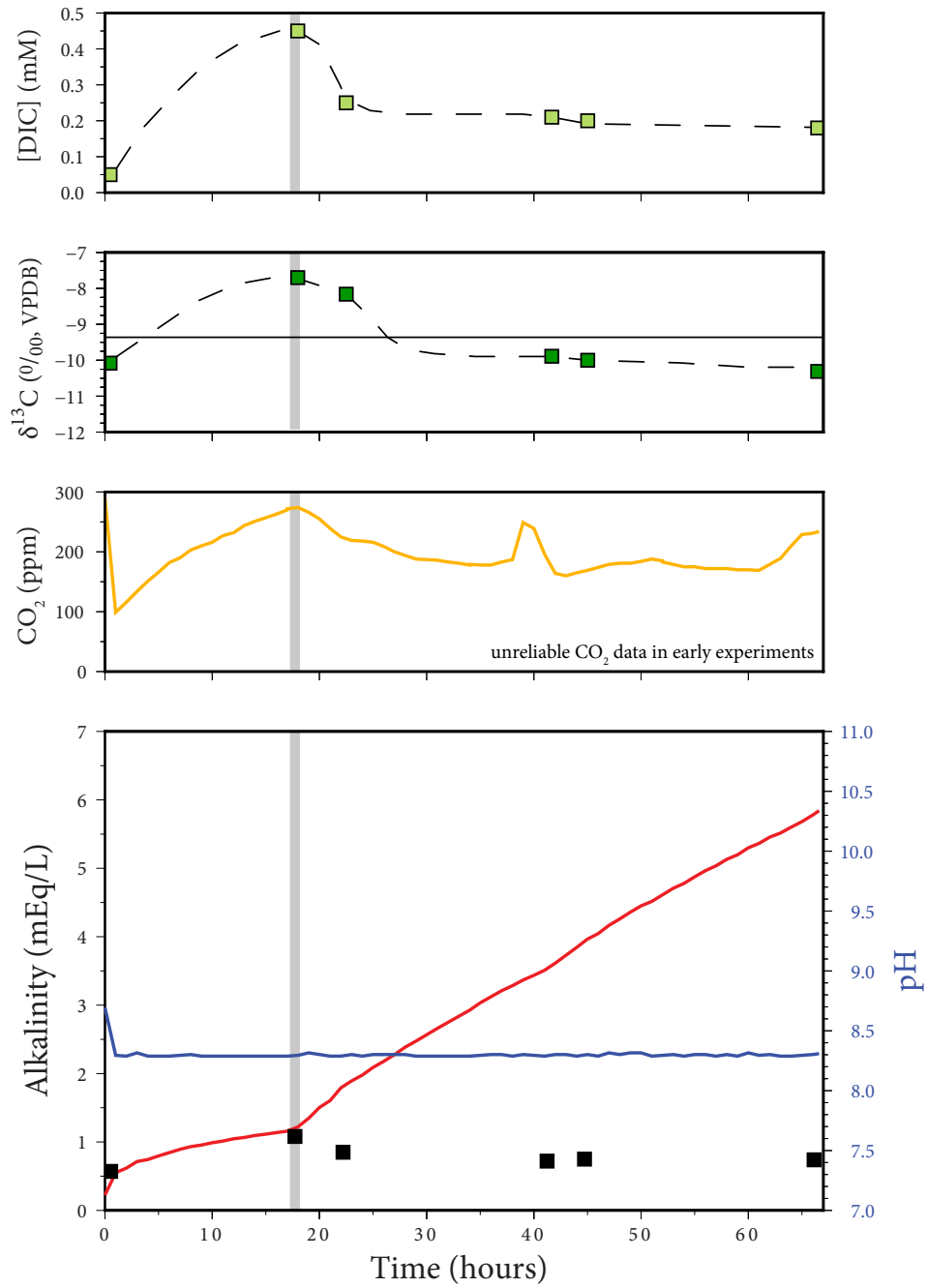


Figure 7: Experiment 3, pH 8.30

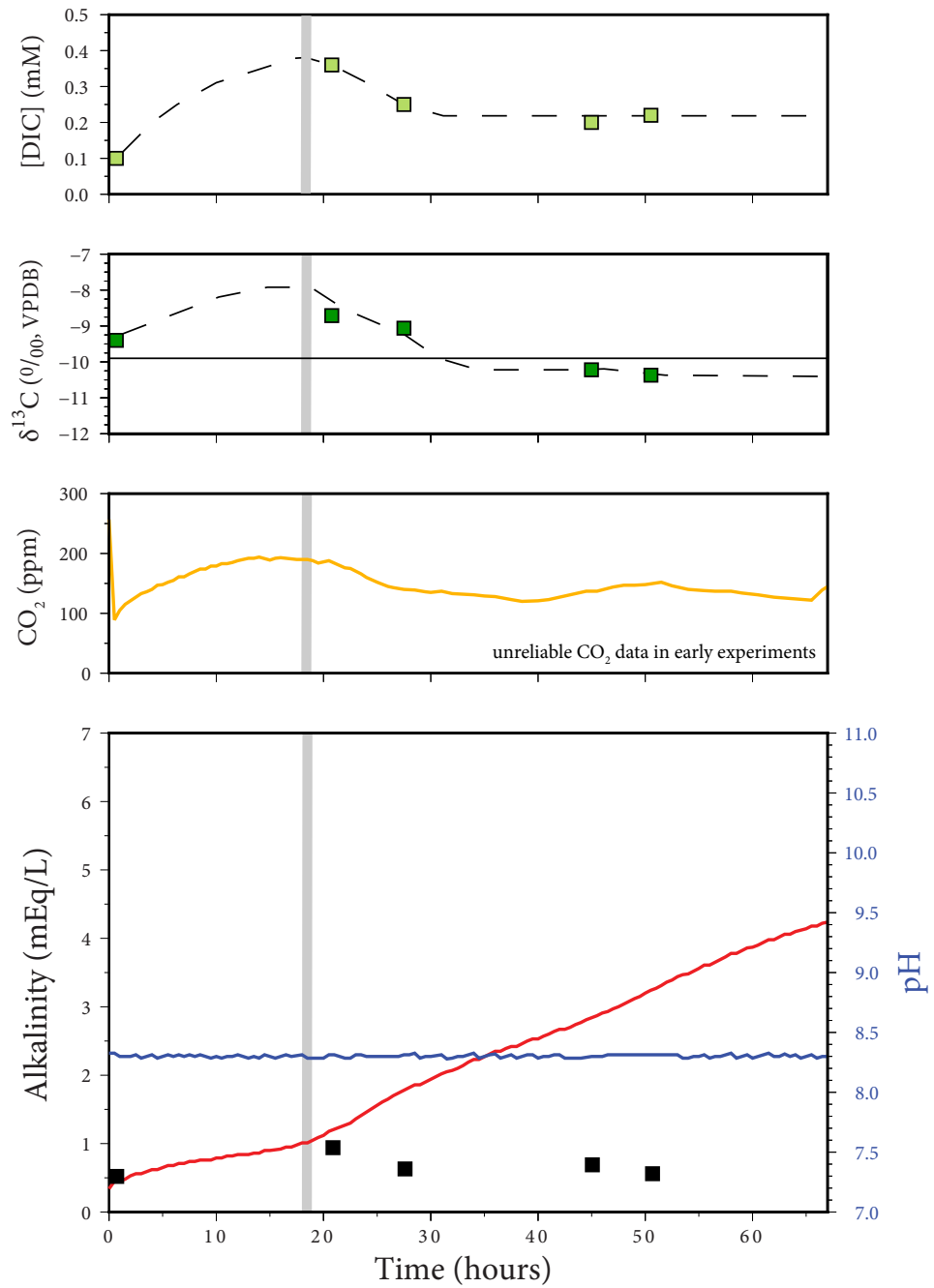


Figure 8: Experiment 4, pH 8.30

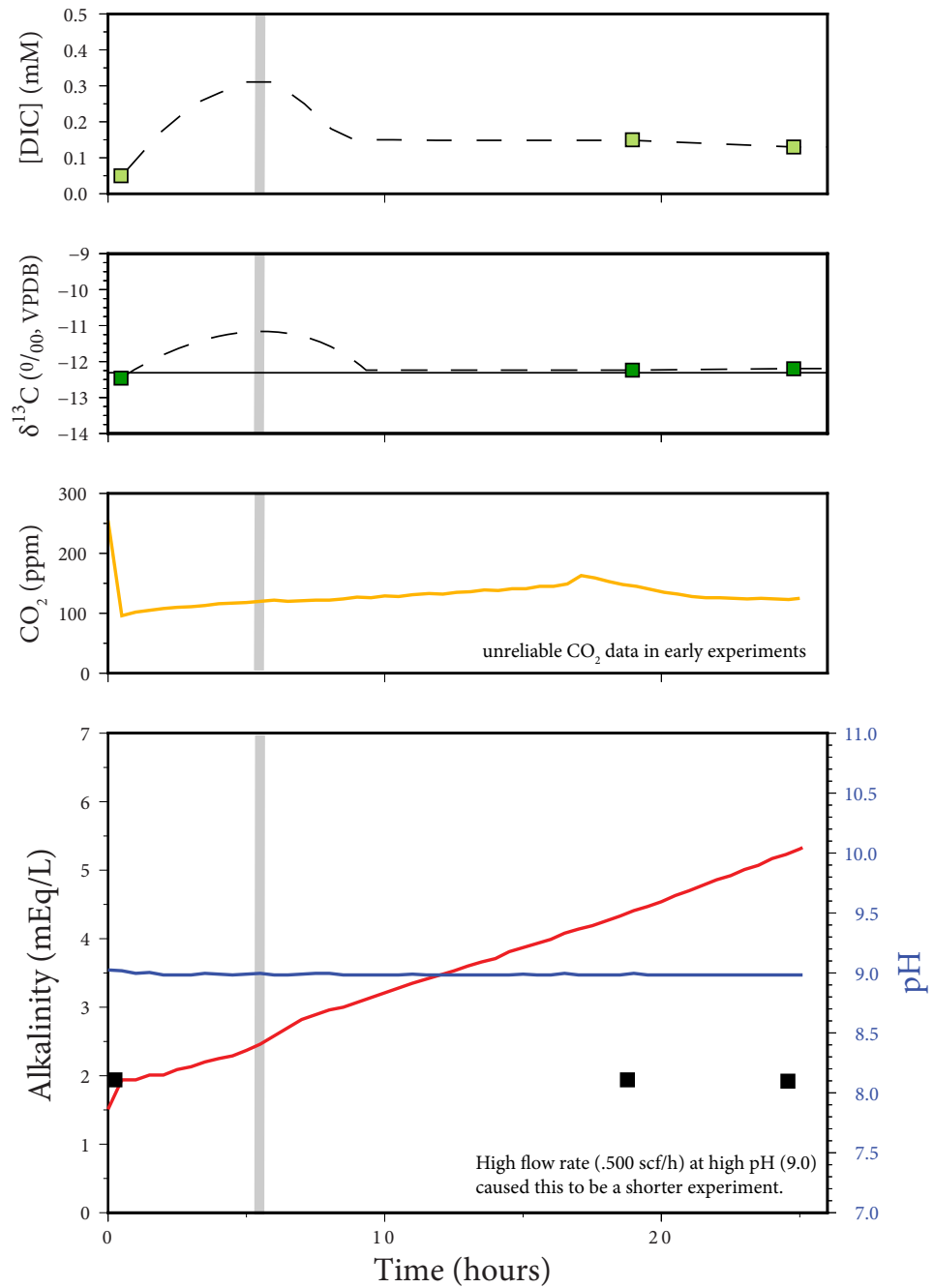


Figure 9: Experiment 5, pH 9.00

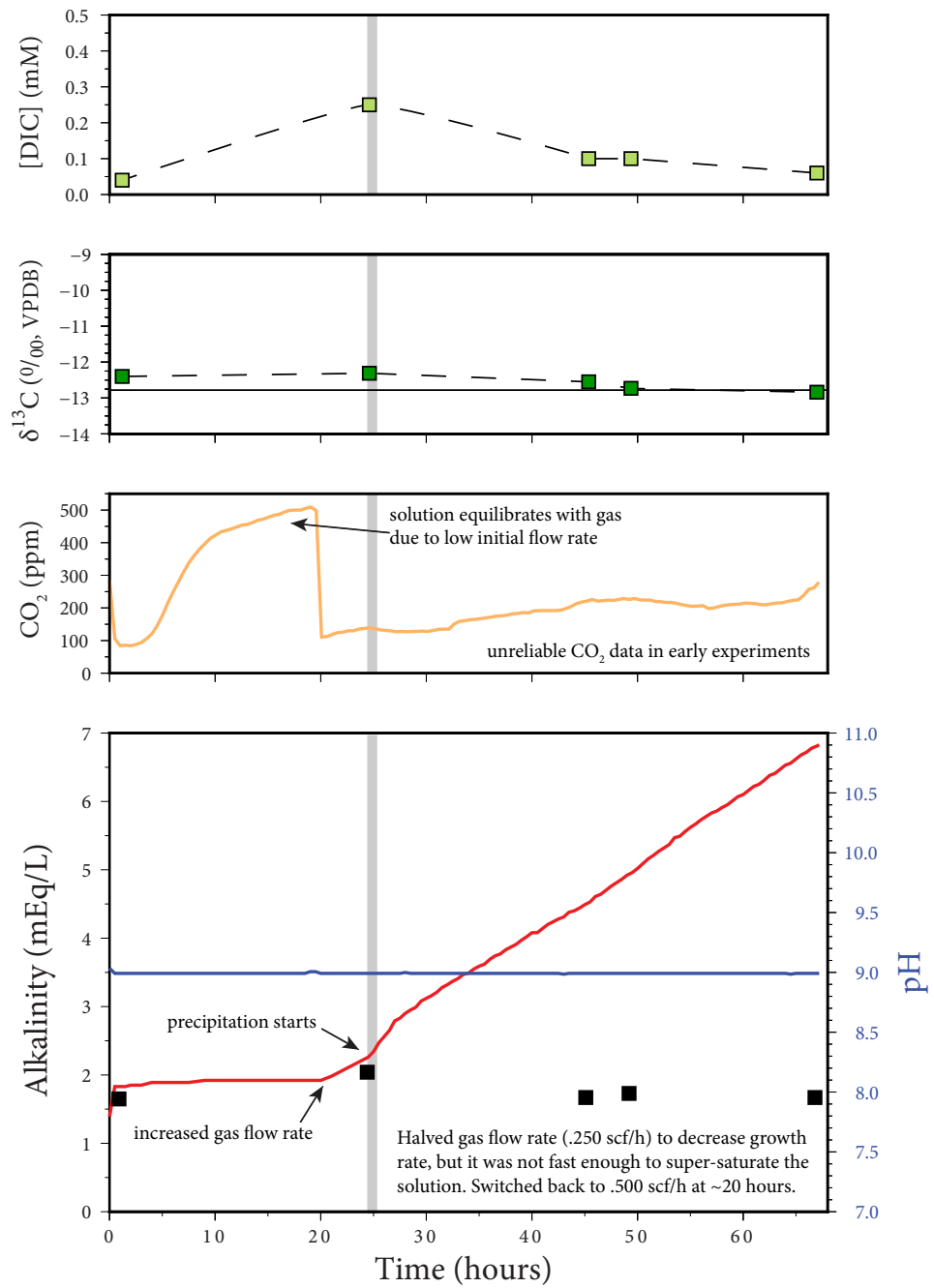


Figure 10: Experiment 6, pH 9.00

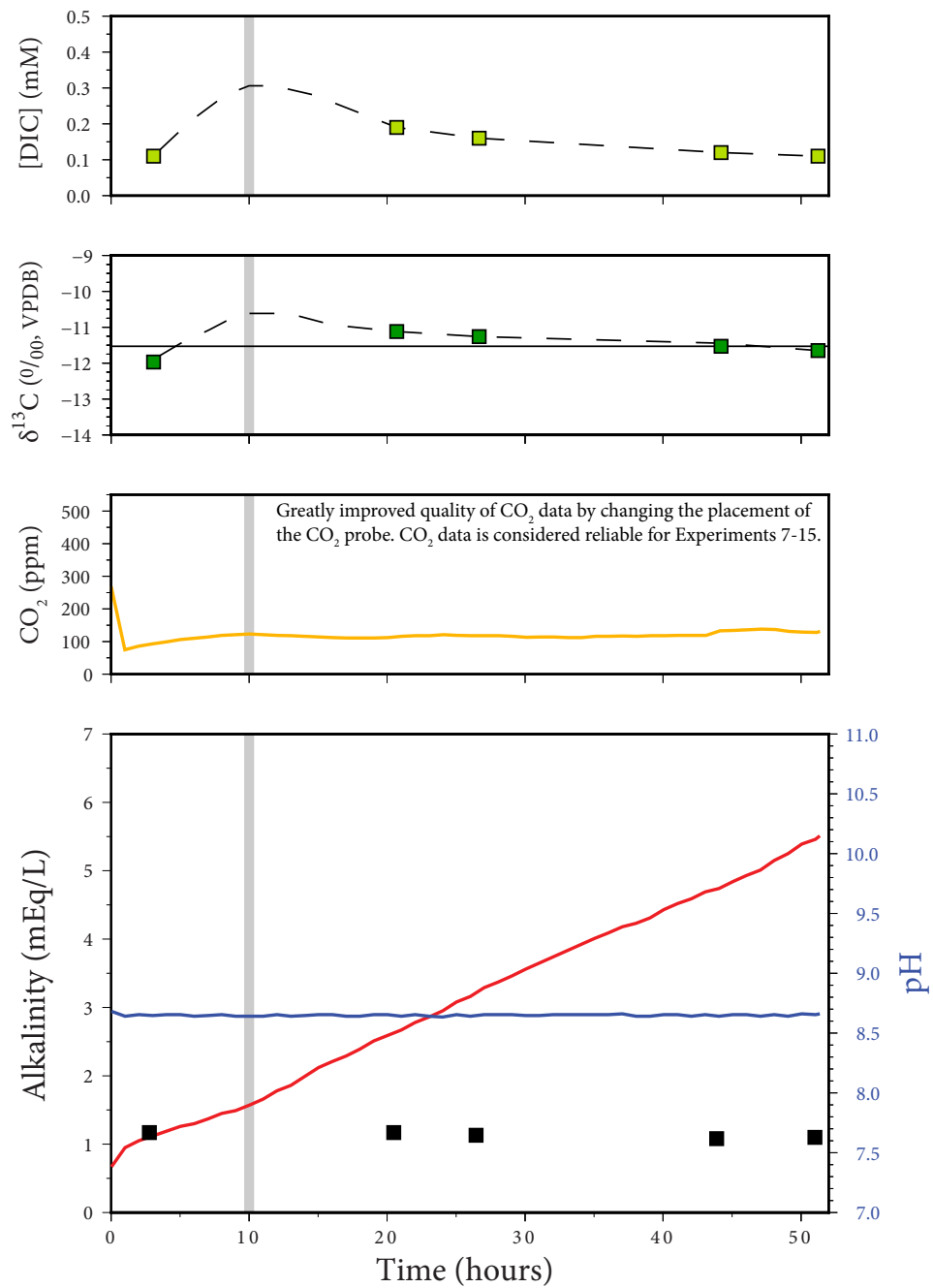


Figure 11: Experiment 7, pH 8.65

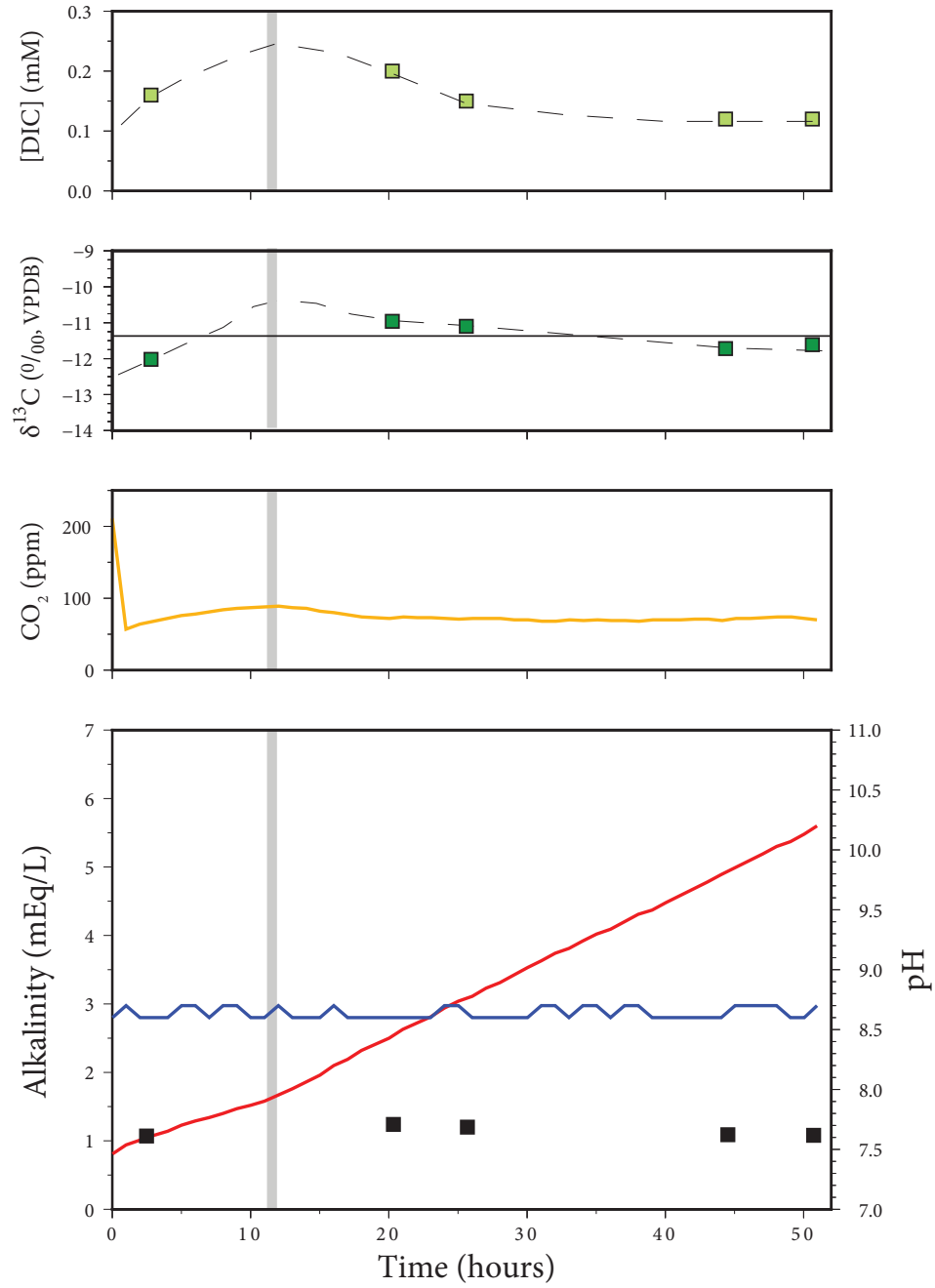


Figure 12: Experiment 8, pH 8.65

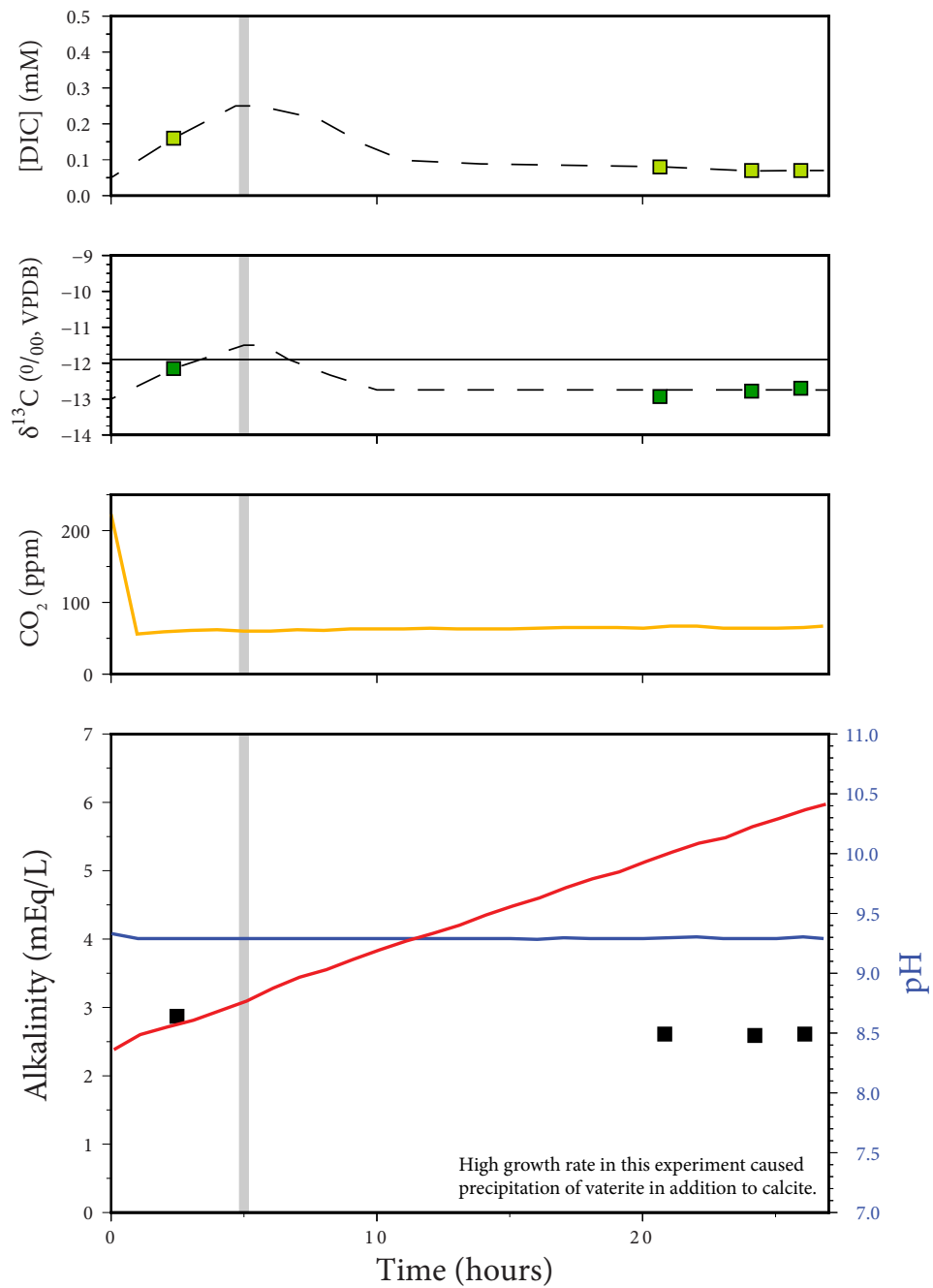


Figure 13: Experiment 9, pH 9.30. Vaterite precipitated along with calcite.

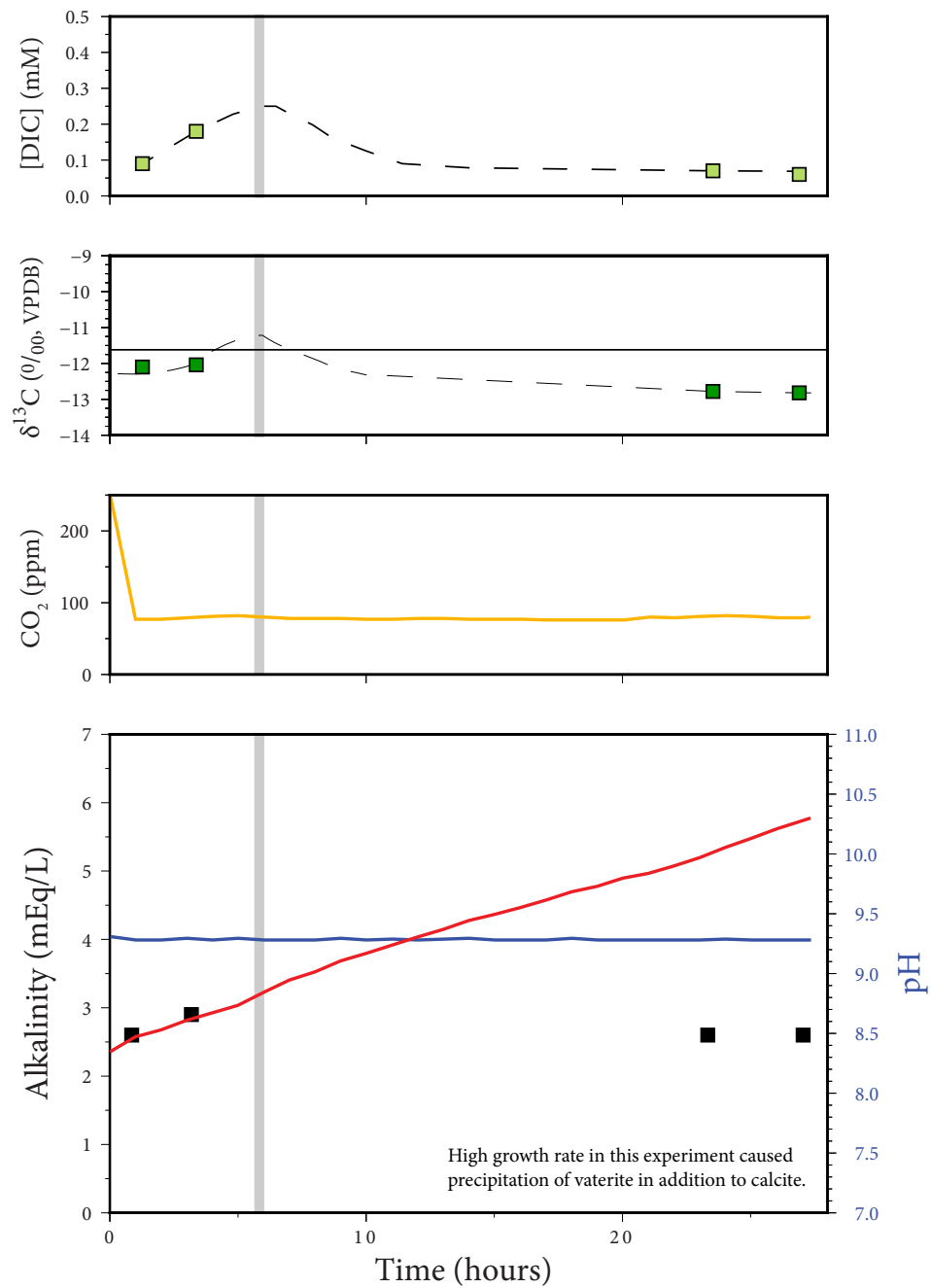


Figure 14: Experiment 10, pH 9.30. Vaterite precipitated along with calcite.

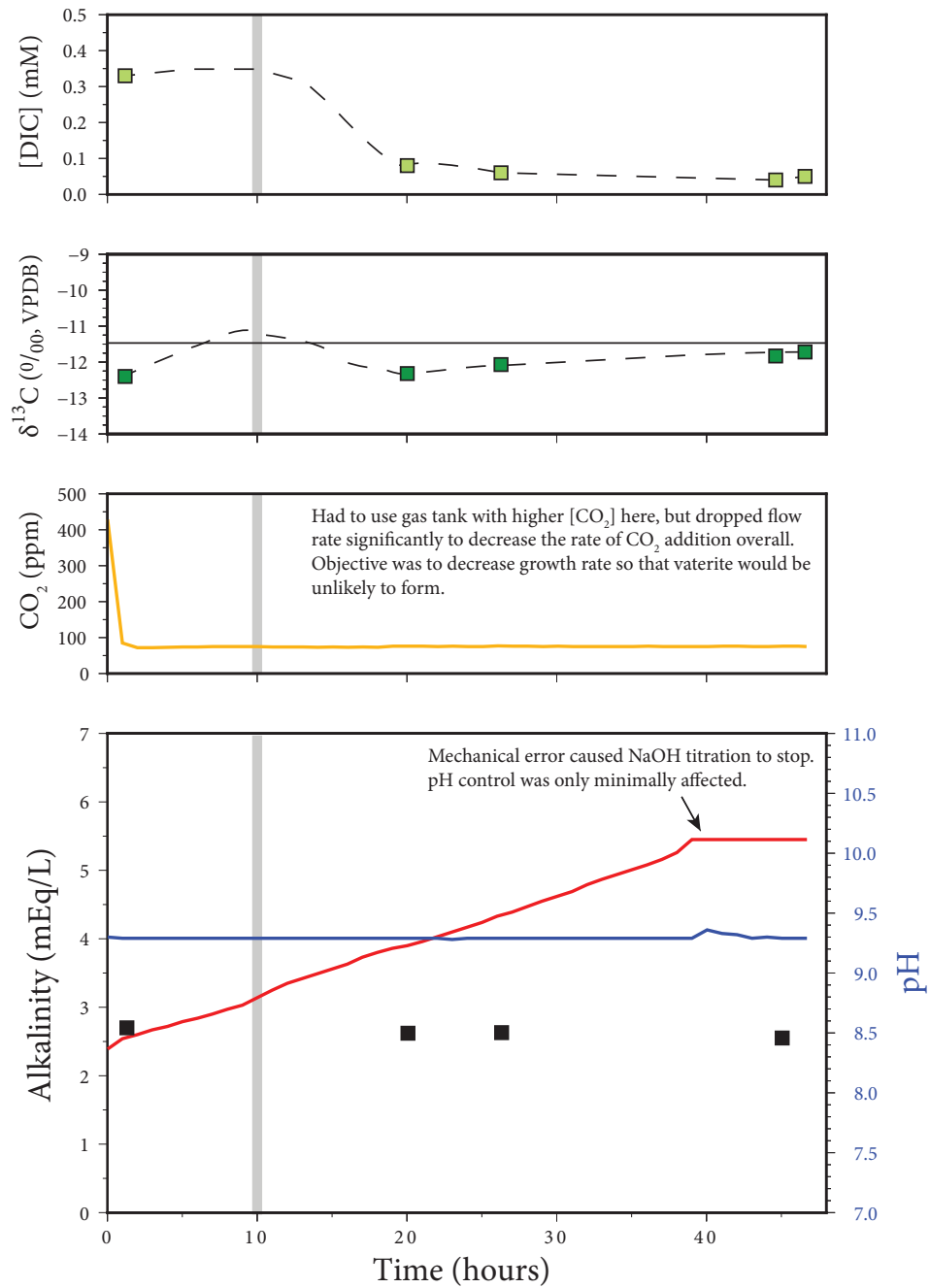


Figure 15: Experiment 11, pH 9.30

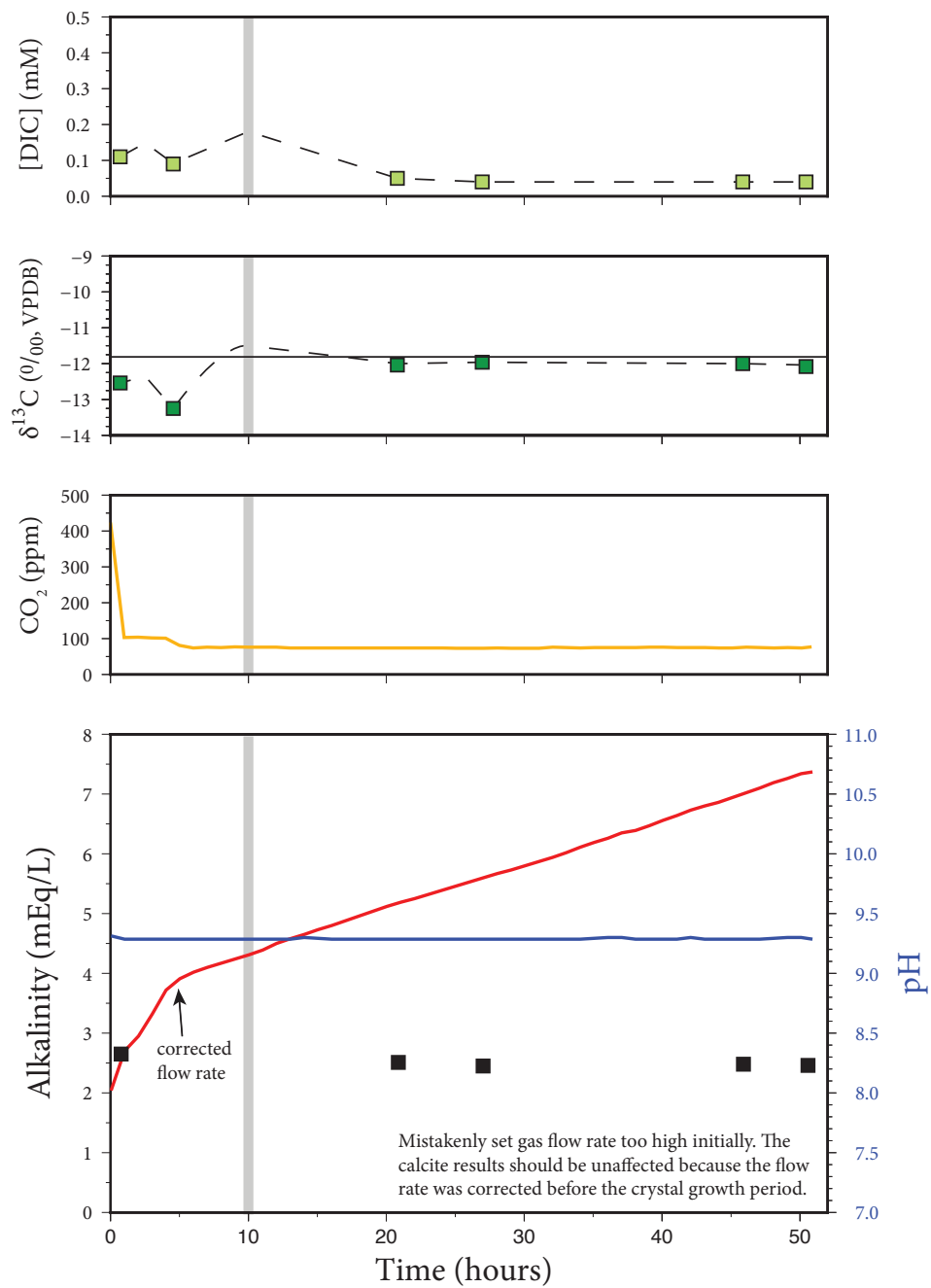


Figure 16: Experiment 12, pH 9.30

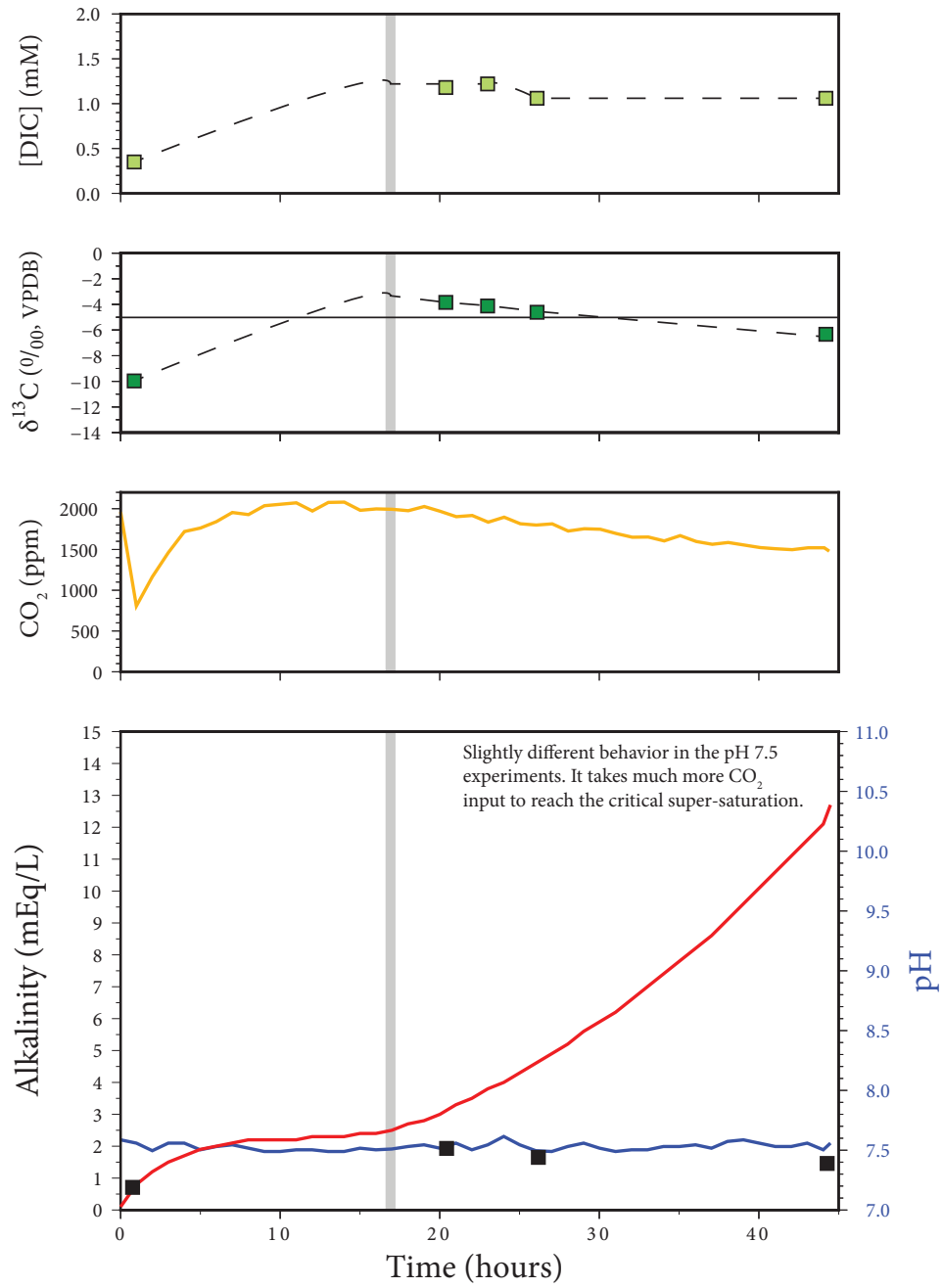


Figure 17: Experiment 14, pH 7.50

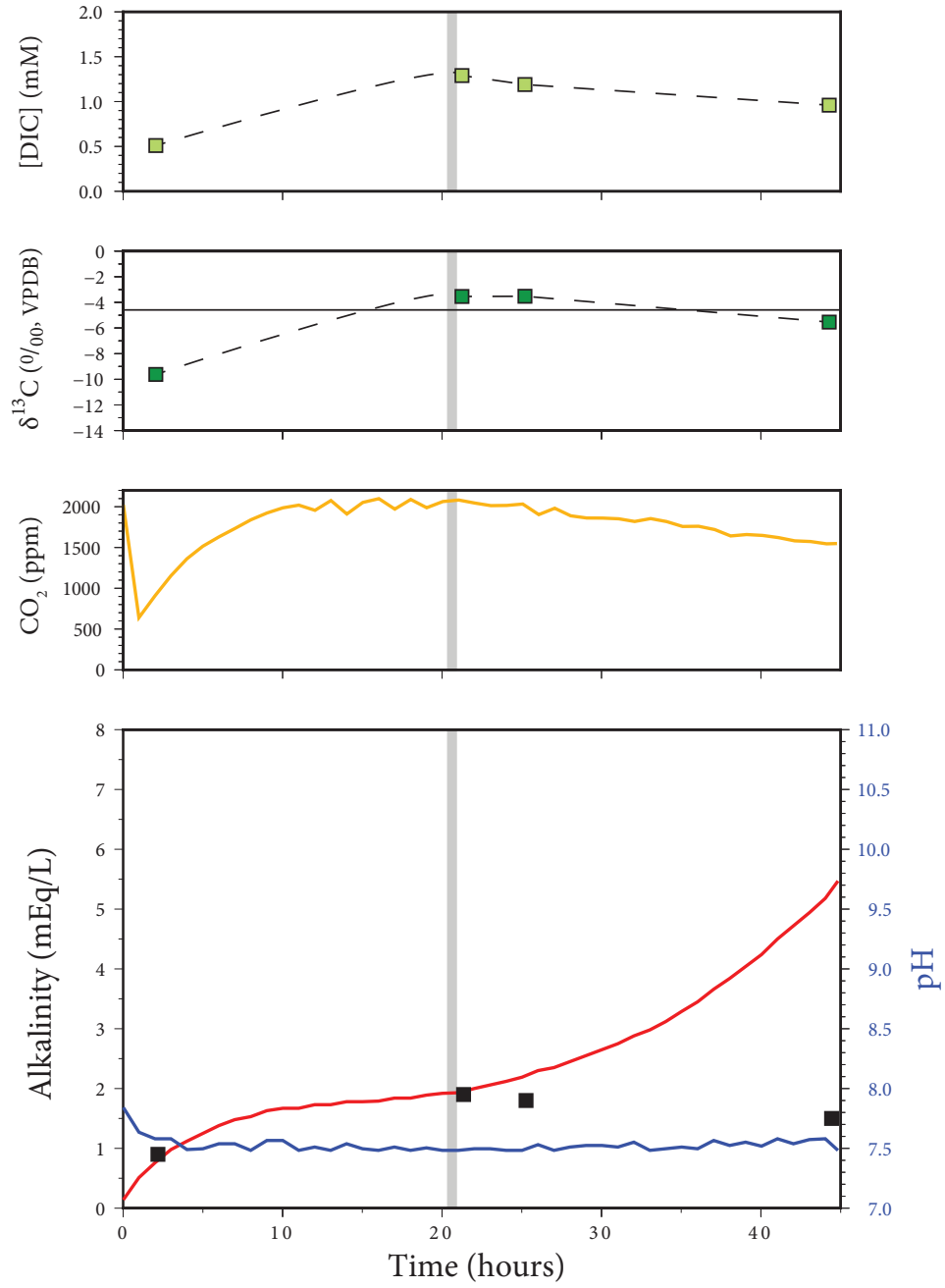
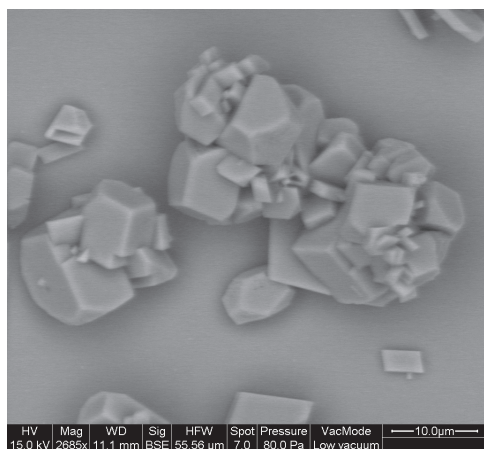
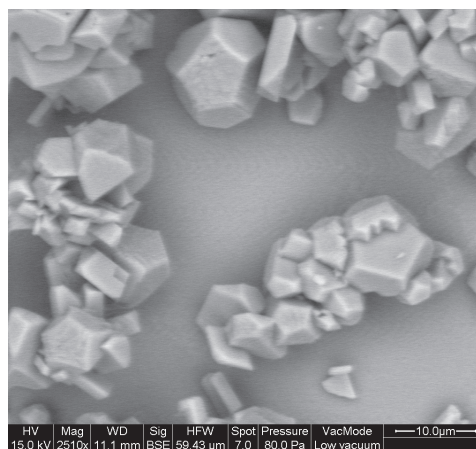


Figure 18: Experiment 15, pH 7.50

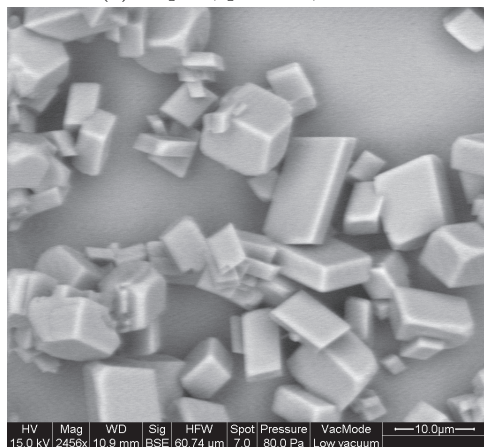
Appendix B: SEM images



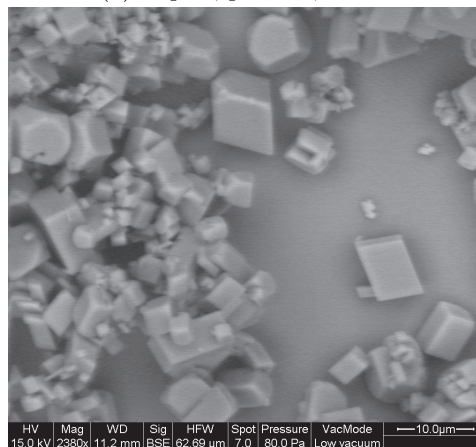
(a) Exp. 3, pH 8.30, calcite



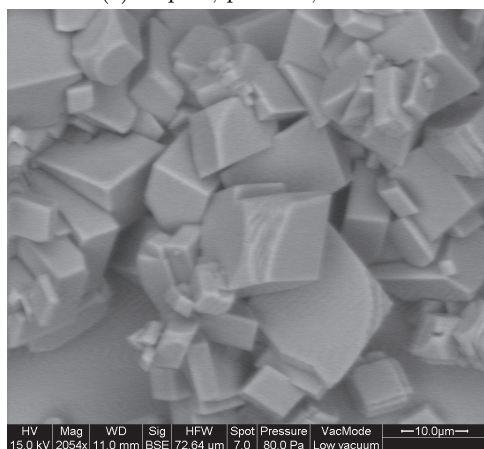
(b) Exp. 4, pH 8.30, calcite



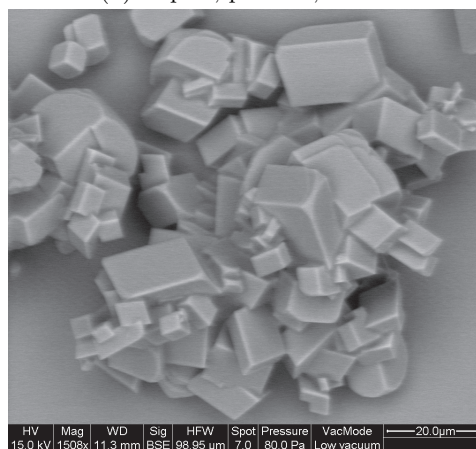
(c) Exp. 5, pH 9.00, calcite



(d) Exp. 6, pH 9.00, calcite

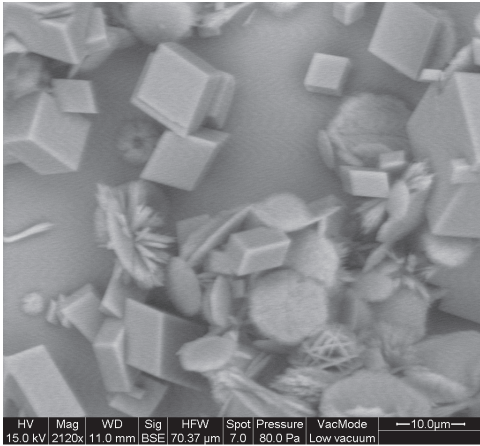


(e) Exp. 7, pH 8.65, calcite

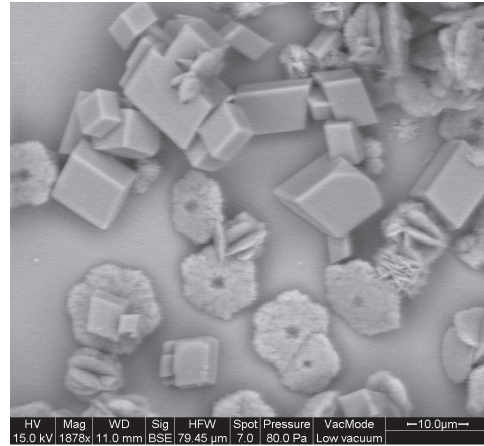


(f) Exp. 8, pH 8.65, calcite

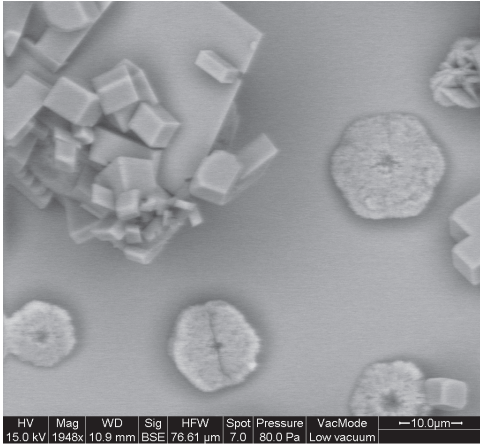
Figure 19: Scanning electron microscope images (back-scattered electrons). Exps. 3-8.



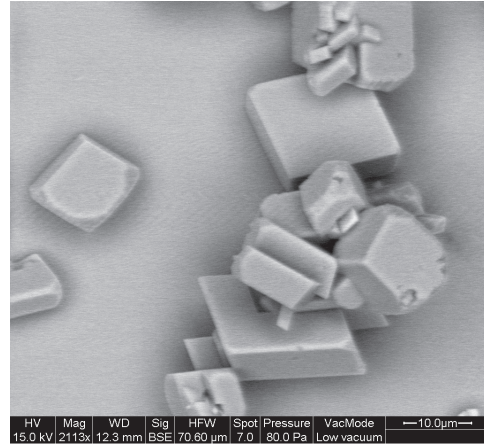
(a) Exp. 9, pH 9.30, calcite and vaterite



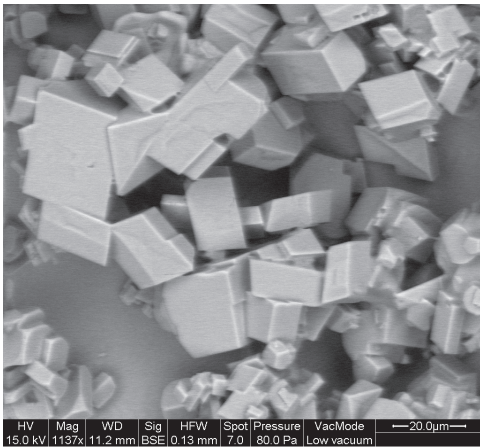
(b) Exp. 10, pH 9.30, calcite and vaterite



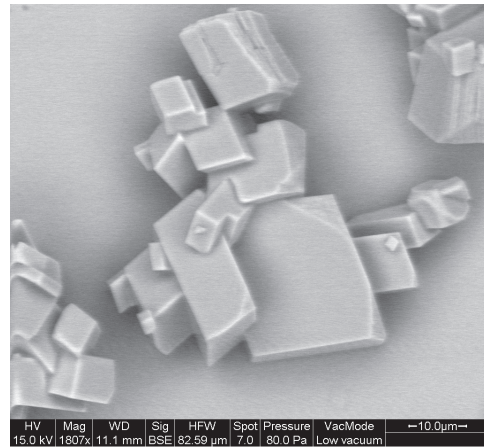
(c) Exp. 11, pH 9.30, calcite and vaterite



(d) Exp. 12, pH 9.30, calcite



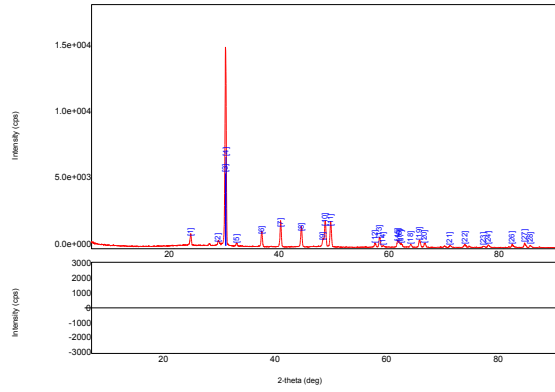
(e) Exp. 14, pH 7.50, calcite



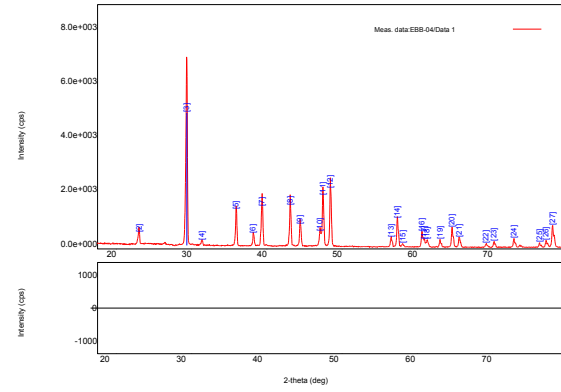
(f) Exp. 15, pH 7.50, calcite

Figure 20: Scanning electron microscope images (back-scattered electrons). Exps. 9-15.

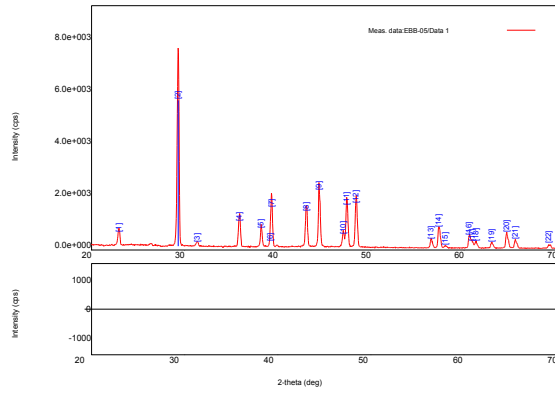
Appendix C: XRD spectra



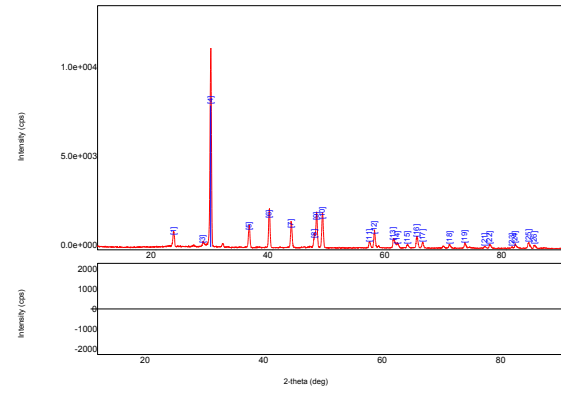
(a) Exp. 3, pH 8.30, calcite



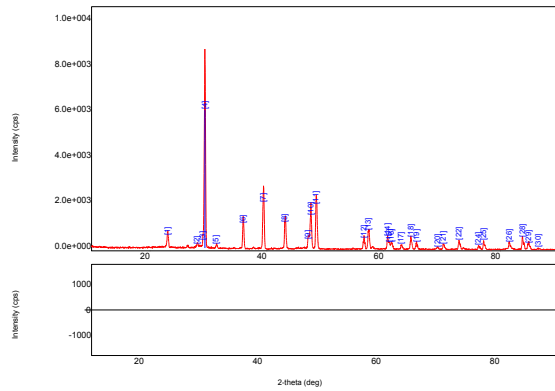
(b) Exp. 4, pH 8.30, calcite



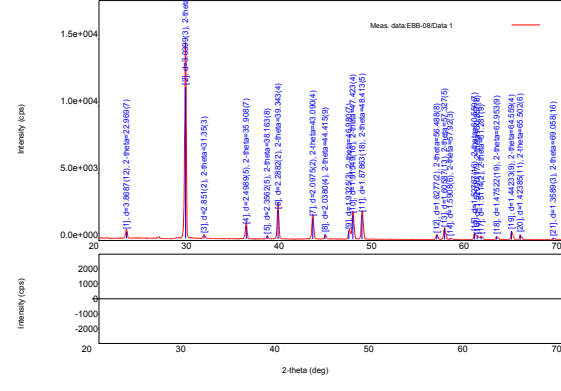
(c) Exp. 5, pH 9.00, calcite



(d) Exp. 6, pH 9.00, calcite

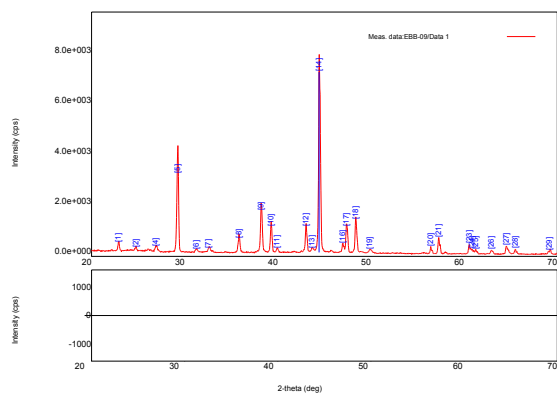


(e) Exp. 7, pH 8.65, calcite

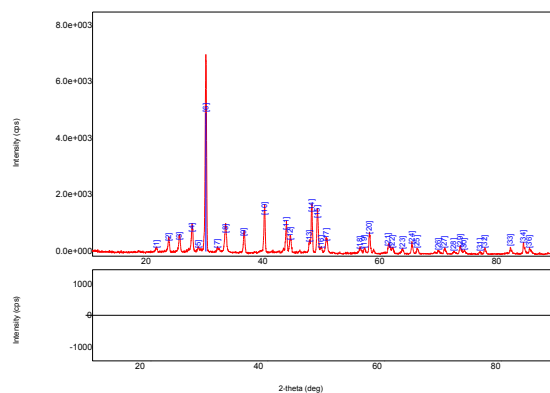


(f) Exp. 8, pH 8.65, calcite

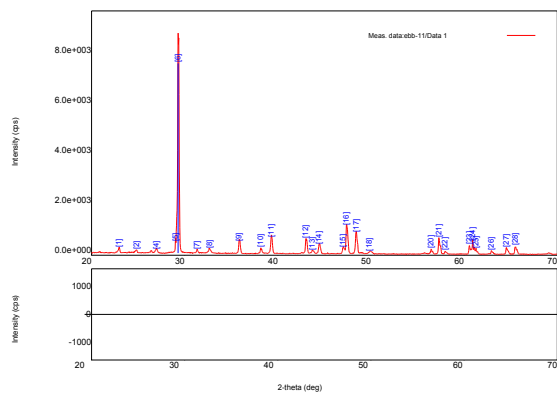
Figure 21: XRD spectra. Exps. 3-8.



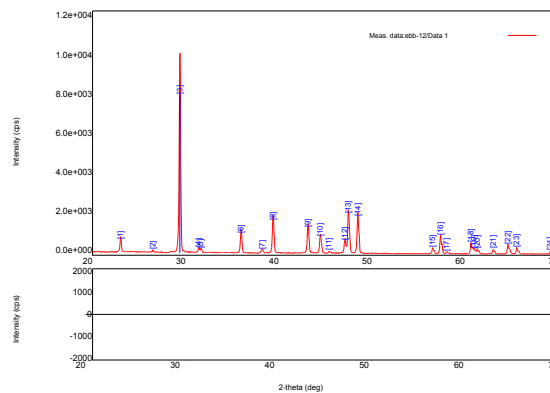
(a) Exp. 9, pH 9.30, calcite and vaterite



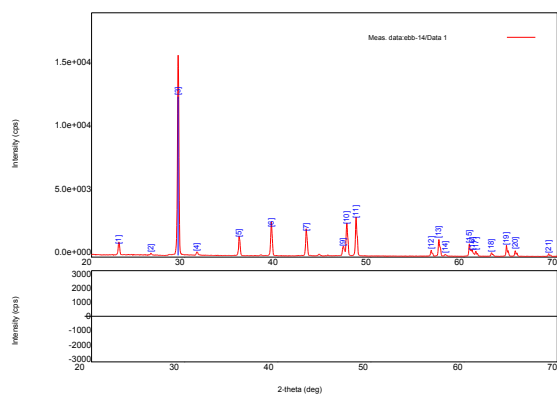
(b) Exp. 10, pH 9.30, calcite and vaterite



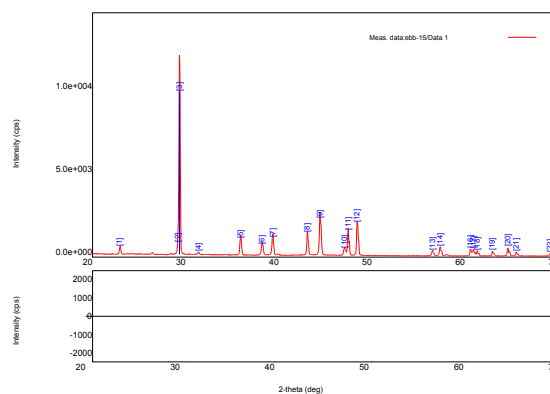
(c) Exp. 11, pH 9.30, calcite and vaterite



(d) Exp. 12, pH 9.30, calcite



(e) Exp. 14, pH 7.50, calcite



(f) Exp. 15, pH 7.50, calcite

Figure 22: XRD spectra. Exps. 9-15.

Appendix D: Uncertainty in carbon isotope fractionation ($\Delta^{13}\text{C}_{\text{xtl-DIC}}$)

A novel feature of our experimental setup is the ability to sample the evolution of $\delta^{13}\text{C}_{\text{DIC}}$ throughout the experiment. This mid-experiment sampling provides an unprecedented level of knowledge about the carbon isotope reservoir from which our crystals are precipitating. However, because we do not continuously monitor the $\delta^{13}\text{C}_{\text{DIC}}$ and because $\delta^{13}\text{C}_{\text{DIC}}$ is not completely constant throughout the experiment, there is still some uncertainty in how to calculate the most accurate $\Delta^{13}\text{C}_{\text{xtl-DIC}}$. This point is illustrated below.

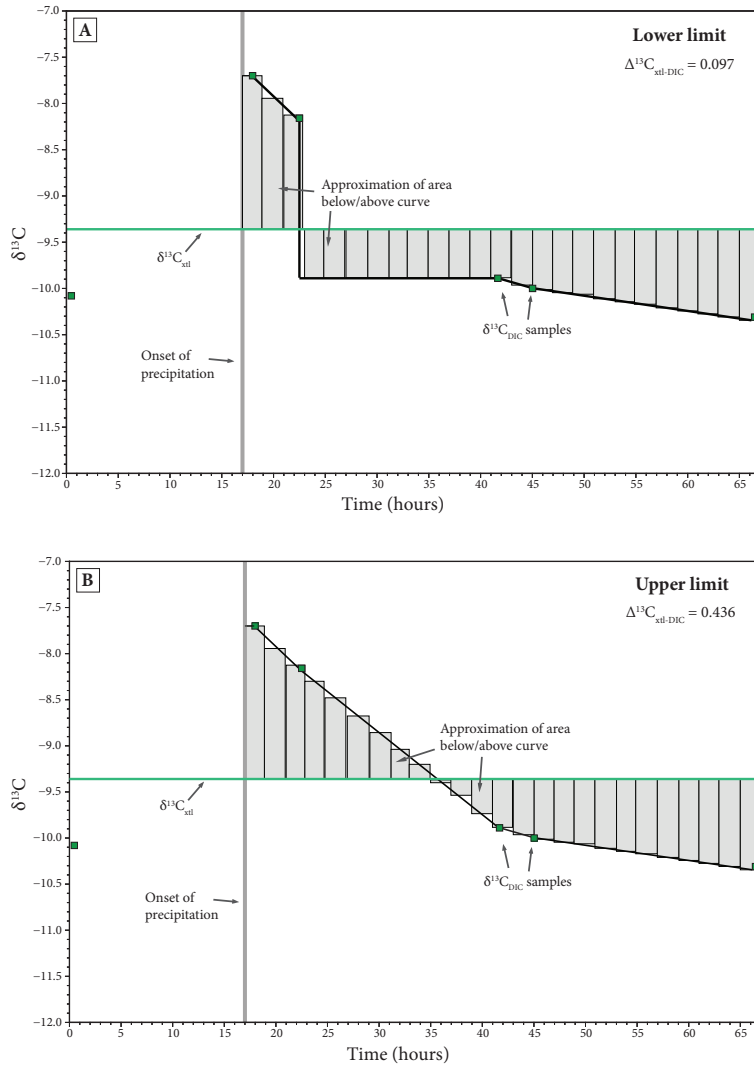


Figure 23: Uncertainty analysis for Experiment 3

The bright green line is $\delta^{13}\text{C}_{\text{xtl}}$ and the dark green squares are our $\delta^{13}\text{C}_{\text{DIC}}$ samples. If we had perfect knowledge of the $\delta^{13}\text{C}_{\text{DIC}}$ -over-time curve, we could calculate $\Delta^{13}\text{C}_{\text{xtl-DIC}}$ by summing the areas between the $\delta^{13}\text{C}_{\text{xtl}}$ line and the $\delta^{13}\text{C}_{\text{DIC}}$ -over-time curve. In our experiments, $\delta^{13}\text{C}_{\text{DIC}}$ is known at the time of each sample but needs to be estimated in between those times. We expect $\delta^{13}\text{C}_{\text{DIC}}$ to decrease fairly rapidly after the onset of precipitation and then stabilize. To determine the range in our $\Delta^{13}\text{C}_{\text{xtl-DIC}}$ calculation, we examine two extreme scenarios for the $\delta^{13}\text{C}_{\text{DIC}}$ evolution. Panel A shows the lower limit for $\Delta^{13}\text{C}_{\text{xtl-DIC}}$, which would occur in the case that $\delta^{13}\text{C}_{\text{DIC}}$ drops off immediately after our sample at $t = 22.5$ hours. Panel B shows the upper limit scenario, in which $\delta^{13}\text{C}_{\text{DIC}}$ decreases linearly between samples at $t = 22.5$ and $t = 41.5$ hours. This indicates that the true $\Delta^{13}\text{C}_{\text{xtl-DIC}}$ is between 0.10 and 0.44‰. We report the average value of 0.27‰ and consider the maximum error to be ± 0.17 ‰.

We used Experiment 3 for the above example because it displays the largest range between the upper and lower limits of $\Delta^{13}\text{C}_{\text{xtl-DIC}}$. When this error analysis was repeated for each experiment, we found that no other experiment had an uncertainty greater than 0.10‰. Considering this in addition to the analytical uncertainty of 0.15‰, we take 0.30‰ to be a general, conservative estimate on the uncertainty in $\Delta^{13}\text{C}_{\text{xtl-DIC}}$. The reproducibility of the results certainly suggests that the true uncertainty may be quite a bit smaller.

REFERENCES CITED

- Adkins, J., Boyle, E., Curry, W., Lutringer, A., 2003. Stable isotopes in deep-sea corals and a new mechanism for “vital effects”. *Geochimica et Cosmochimica Acta* 67 (6), 1129–1143.
- Affek, H. P., 2013. Clumped isotopic equilibrium and the rate of isotope exchange between CO₂ and water. *American Journal of Science* 313 (4), 309–325.
- Beck, W. C., Grossman, E. L., Morse, J. W., 2005. Experimental studies of oxygen isotope fractionation in the carbonic acid system at 15°, 25°, and 40°C. *Geochimica et Cosmochimica Acta* 69 (14), 3493–3503.
- Bottinga, Y., 1968. Calculation of fractionation factors for carbon and oxygen isotopic exchange in the system calcite-carbon dioxide-water. *The Journal of Physical Chemistry* 72 (3), 800–808.
- Carpenter, S. J., Lohmann, K. C., 1995. $\delta^{18}\text{O}$ and $\delta^{13}\text{C}$ values of modern brachiopod shells. *Geochimica et Cosmochimica Acta* 59 (18), 3749–3764.
- Coplen, T. B., 2007. Calibration of the calcite–water oxygen-isotope geothermometer at Devils Hole, Nevada, a natural laboratory. *Geochimica et Cosmochimica Acta* 71 (16), 3948–3957.
- Deines, P., 2005. Comment on “An explanation of the effect of seawater carbonate concentration on foraminiferal oxygen isotopes,” by RE Zeebe (1999). *Geochimica et Cosmochimica Acta* 69 (3), 787.
- Dennis, K. J., Schrag, D. P., 2010. Clumped isotope thermometry of carbonatites as an indicator of diagenetic alteration. *Geochimica et Cosmochimica Acta* 74 (14), 4110–4122.
- Dietzel, M., Tang, J., Leis, A., Köhler, S. J., 2009. Oxygen isotopic fractionation during inorganic calcite precipitation – Effects of temperature, precipitation rate and pH. *Chemical Geology* 268 (1), 107–115.
- Eiler, J. M., 2007. ‘Clumped-isotope’ geochemistry – The study of naturally-occurring, multiply-substituted isotopologues. *Earth and Planetary Science Letters* 262 (3), 309–327.
- Eiler, J. M., 2011. Paleoclimate reconstruction using carbonate clumped isotope thermometry. *Quaternary Science Reviews* 30 (25), 3575–3588.
- Ghosh, P., Adkins, J., Affek, H., Balta, B., Guo, W., Schauble, E. A., Schrag, D., Eiler, J. M., 2006. ^{13}C – ^{18}O bonds in carbonate minerals: A new kind of paleothermometer. *Geochimica et Cosmochimica Acta* 70 (6), 1439–1456.
- Kim, S.-T., O’Neil, J. R., 1997. Equilibrium and nonequilibrium oxygen isotope effects in synthetic carbonates. *Geochimica et Cosmochimica Acta* 61 (16), 3461–3475.

- Kupriyanova, E., Pronina, N., 2011. Carbonic anhydrase: enzyme that has transformed the biosphere. *Russian Journal of Plant Physiology* 58 (2), 197–209.
- McConnaughey, T., 1989a. ^{13}C and ^{18}O isotopic disequilibrium in biological carbonates: I. Patterns. *Geochimica et Cosmochimica Acta* 53 (1), 151–162.
- McConnaughey, T., 1989b. ^{13}C and ^{18}O isotopic disequilibrium in biological carbonates: II. *In vitro* simulation of kinetic isotope effects. *Geochimica et Cosmochimica Acta* 53 (1), 163–171.
- McCrea, J. M., 1950. On the isotopic chemistry of carbonates and a paleotemperature scale. *The Journal of Chemical Physics* 18 (6), 849–857.
- Romanek, C. S., Grossman, E. L., Morse, J. W., 1992. Carbon isotopic fractionation in synthetic aragonite and calcite: effects of temperature and precipitation rate. *Geochimica et Cosmochimica Acta* 56 (1), 419–430.
- Spero, H. J., Bijma, J., Lea, D. W., Bemis, B. E., 1997. Effect of seawater carbonate concentration on foraminiferal carbon and oxygen isotopes. *Nature* 390 (6659), 497–500.
- Tang, J., Dietzel, M., Fernandez, A., Tripathi, A. K., Rosenheim, B. E., 2014. Evaluation of kinetic effects on clumped isotope fractionation ($\delta 47$) during inorganic calcite precipitation. *Geochimica et Cosmochimica Acta* 134, 120–136.
- Tarutani, T., Clayton, R. N., Mayeda, T. K., 1969. The effect of polymorphism and magnesium substitution on oxygen isotope fractionation between calcium carbonate and water. *Geochimica et Cosmochimica Acta* 33 (8), 987–996.
- Uchikawa, J., Zeebe, R. E., 2012. The effect of carbonic anhydrase on the kinetics and equilibrium of the oxygen isotope exchange in the $\text{CO}_2\text{--H}_2\text{O}$ system: Implications for $\delta^{18}\text{O}$ vital effects in biogenic carbonates. *Geochimica et Cosmochimica Acta* 95, 15–34.
- Urey, H. C., 1947. The thermodynamic properties of isotopic substances. *J. Chem. Soc.*, 562–581.
- Usdowski, E., Hoefs, J., 1993. Oxygen isotope exchange between carbonic acid, bicarbonate, carbonate, and water: a re-examination of the data of McCrea (1950) and an expression for the overall partitioning of oxygen isotopes between the carbonate species and water. *Geochimica et Cosmochimica Acta* 57 (15), 3815–3818.
- Watkins, J. M., Hunt, J. D., Ryerson, F. J., DePaolo, D. J., 2014. The influence of temperature, pH, and growth rate on the $\delta^{18}\text{O}$ composition of inorganically precipitated calcite. *Earth and Planetary Science Letters* 404, 332–343.
- Watkins, J. M., Nielsen, L. C., Ryerson, F. J., DePaolo, D. J., 2013. The influence of kinetics on the oxygen isotope composition of calcium carbonate. *Earth and Planetary Science Letters* 375, 349–360.

- Watson, E. B., 2004. A conceptual model for near-surface kinetic controls on the trace-element and stable isotope composition of abiogenic calcite crystals. *Geochimica et Cosmochimica Acta* 68 (7), 1473–1488.
- Wolthers, M., Nehrke, G., Gustafsson, J. P., Van Cappellen, P., 2012. Calcite growth kinetics: Modeling the effect of solution stoichiometry. *Geochimica et Cosmochimica Acta* 77, 121–134.
- Zaarur, S., Affek, H. P., Brandon, M. T., 2013. A revised calibration of the clumped isotope thermometer. *Earth and Planetary Science Letters* 382, 47–57.
- Zeebe, R., 2007. An expression for the overall oxygen isotope fractionation between the sum of dissolved inorganic carbon and water. *Geochemistry, Geophysics, Geosystems* 8 (9).
- Zeebe, R. E., 2001. Seawater pH and isotopic paleotemperatures of cretaceous oceans. *Palaeogeography, Palaeoclimatology, Palaeoecology* 170 (1), 49–57.
- Zeebe, R. E., Wolf-Gladrow, D., Jansen, H., 1999. On the time required to establish chemical and isotopic equilibrium in the carbon dioxide system in seawater. *Marine Chemistry* 65 (3), 135–153.
- Zeebe, R. E., Wolf-Gladrow, D. A., 2001. CO₂ in seawater: equilibrium, kinetics, isotopes. Vol. 65. Gulf Professional Publishing.